

Supernumerary Robotic Limbs for Human Augmentation in Overhead Assembly Tasks

by

Lawrence "Zack" Bright

Submitted to the Department of Mechanical Engineering
in partial fulfillment of the requirements for the degree of

Master of Science in Mechanical Engineering

at the

MASSACHUSETTS INSTITUTE OF TECHNOLOGY

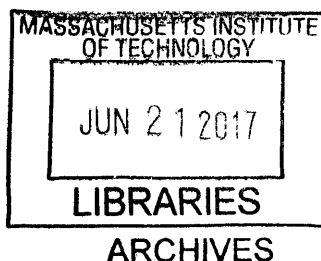
June 2017

© Massachusetts Institute of Technology 2017. All rights reserved.

Author  Signature redacted
.....
Department of Mechanical Engineering
May 12, 2017

Certified by Signature redacted
.....
H. Harry Asada
Ford Professor of Mechanical Engineering
Thesis Supervisor

Accepted by Signature redacted
.....
Rohan Abeyaratne
Quentin Berg Professor of Mechanics
Graduate Officer



Supernumerary Robotic Limbs for Human Augmentation in Overhead Assembly Tasks

by

Lawrence "Zack" Bright

Submitted to the Department of Mechanical Engineering
on May 12, 2017, in partial fulfillment of the
requirements for the degree of
Master of Science in Mechanical Engineering

Abstract

Manufacturing tasks are highly demanding of work, and there is an especially high prevalence of injury associated with overhead tasks which are taxing to the shoulder and upper body. To assist workers completing these tasks, and to increase overall productivity, safety and effectiveness, we introduce a novel design of Supernumerary Robotic Limb (SRL). This is a robotic arm worn on the shoulder of the technician/-worker which extends the human capability with implicit force control algorithms that allow for intuitive control and interface of the extra robot arm. Affectionately dubbed Aucto, the robotic arm can lift an object and hold it while the wearer is securing the object using a tool with both hands. The worker does not have to take a laborious posture for a long time, reducing fatigue and injuries. Furthermore, a single worker can execute the task, which would otherwise require two workers. Two technical challenges and novel solutions are presented. One is to make the wearable robot simple and lightweight with use of a new type of granular jamming gripper that can grasp diverse objects from an arbitrary direction. This eliminates the need for orienting the gripper against the object with three-axis wrist joints, reducing the number of degrees of freedom (DOF) from 6 to 3. The other is an effective control algorithm that allows the wearer to move freely while the robot on the shoulder is holding an object. Unlike a robot sitting on a floor, the SRL worn by a human is disturbed by the movement of the wearer. An admittance-based control algorithm allows the robot to hold the object stably and securely despite the human movement and changes in posture. A 3 DOF prototype robot with a new granular jamming gripper and an ergonomic body mounting gear is developed and tested. It is demonstrated that the robot can hold a large object securely in the overhead area despite the movement of the wearer while performing an assembly work.

Thesis Supervisor: H. Harry Asada
Title: Ford Professor of Mechanical Engineering

Acknowledgments

I begin my thanks first and foremost with Emma. You have been my rock, a shining beacon in the storm, and best of all, my source of hope and inspiration. This has been a long journey with many twists and turns and I trust we will look back on it with fondness and nostalgia, despite the challenges.

To my family, all of you, I thank you for the guidance, long calls, boastful pride in me, and an immense wealth of love that held me up against my own self-doubt. I am proud to have accomplished so very much and will always try my hardest to make you proud.

To my friends, brothers, and many colleagues at MIT, there are almost too many of you to count, but I hope that I gave you enough praise and thanks in the moment. I cannot enumerate in these pages how lucky I am to have been able to surround myself with the best that MIT has to offer. My experiences shared with you have made me who I am – all for the better I believe. I take a little bit of each of you with me forward, knowing that we will hopefully cross paths time and time again.

To those of you in the d'Arbelloff lab, I am so grateful to have in you all, the best of mentors, friends, teammates, and classmates. I cannot imagine my MIT graduate experience without you. You are each in your own right some of the best engineers, biologists, scientists, and roboticists that I have had the pleasure of encountering in the world, and more than that, you count among yourselves some of the most openhearted and dedicated people that I have know. Through the good times and bad, I always knew I could count on you all.

To Professor Asada, I am so very grateful for your guidance throughout my time as your student, you have been an invaluable resource of advice, knowledge and motivation to keep working hard. Your insight, ideas, work ethic, and creativity are all examples I strive toward. I thank you most of all for the great opportunity to have done so much in so little time.

To anyone and everyone I have crossed paths with at MIT, I say thank you for in your own way bringing me to this point in my life.

Contents

1	Introduction	15
1.1	Task Motivation, Overhead Assembly in Manufacturing	15
1.2	Overview of Work enclosed	17
2	Design Concepts	19
2.1	Guiding Design Principles	19
2.1.1	Safety	19
2.1.2	Flexibility	20
2.1.3	Ergonomics	20
2.1.4	Simplicity	21
2.2	Wearable Robots	21
2.3	Supernumerary Robotic Limbs	21
2.4	Functional Requirements	22
2.5	SRL for Overhead Tasks	22
2.6	Use of a Granular Jamming Gripper	24
3	Human Intent Sensing and Modeling	27
3.1	Sensing Human Task Execution and Intent	29
3.1.1	Sensing Motion	29
3.1.2	Sensing Posture and Orientation	30
3.1.3	Sensing Intent and Focus with Eyetracking	32
3.2	Task Modeling	34
3.2.1	Colored Petri Nets	35

3.3	Statistical Modeling	35
3.3.1	POMDP Models	36
3.3.2	POMDP Software	37
3.4	Control from Redundant Degrees of Freedom	37
3.4.1	Neural Network Sensor Suit Concept - Redundant Shoulder Control	39
3.5	Sensing Human Fatigue and Human Fatigue Modeling	40
4	Human-Machine Mounting Interface	41
4.1	Worn Robot Mounting	41
4.2	ExoSuit Concept	43
4.2.1	Comparing to Other Systems	44
4.2.2	Fabrication	45
4.2.3	Testing and Iterating	46
5	Mechanical Design and Electronics	49
5.1	Robotic Arm Design	49
5.1.1	Kinematic Structure	49
5.1.2	Initial and Previous Implementations	50
5.1.3	Final Implementation of Mechanical Design	53
5.2	Electronics, Sensors, and Low Level Software	55
5.2.1	Force Sensor	59
5.3	Universal Gripper Design	60
6	Controls System	67
6.1	Control Laws and Algorithms	67
6.1.1	Coordinate Systems and Motion Compensation	67
6.1.2	Torque Control of SRL	70
6.1.3	Admittance Control for SRL	72
6.1.4	Final Algorithm Implementation	75

7	Testing, Results and Performance	79
7.1	Testing-Experimental Procedure	79
7.1.1	Human Haptic Feedback and Proprioception	82
7.2	Force Control Tracking and Holding	82
7.3	Admittance Tuning	83
7.4	Postural Compensation and Tracking of the World Coordinates . . .	85
8	Conclusion and Future Works	89

List of Figures

1-1	Workers Completing Overhead Tasks in Aircraft Assembly – Snapshot of video of Boeing 787-9 Dreamliner Assembly [2]	16
1-2	Final Version of Aucto being worn, shown from front and back	18
2-1	A person completing an overhead task with the SRL	23
2-2	SRL Kinematic Structure	24
2-3	SRL Workspace with model of a person and the human arm workspace	25
2-4	Granular Jamming Gripper can grasp objects from an arbitrary direction, eliminating the need for a powered wrist	26
3-1	Mounting locations of all the IMUs in the sensor suit concept	30
3-2	BNO055 sensor packages inside custom cases which allow attachment via strap, adhesive, sewing, and other methods, though this is what had been employed.	31
3-3	Colored Petri Net Model developed by Llorens et. al [19], shown is as well the compiled state machine of the CPN.	36
4-1	Prototype of the Ergonomic body attachment or "ExoSuit"	42
4-2	The structural loop of the new ergonomic attachment vs. a standard exoskeleton or person	43
4-3	The base of the SRL is insert molded into the stiff shoulder platform of the ExoSuit	46
4-4	Instamorph of the ExoSuit cooling; transparent when plastic, opaque when set as "glass"	47

4-5	The Process of heating the instamorph to prepare it for molding: heating until thermoplastic	47
4-6	Tennis Ball Mounting used in the intial proprioception trials	48
2-2	SRL Kinematic Structure, repeated for reference	50
2-3	SRL Workspace with model of a person and the human arm workspace, repeated for reference	50
5-3	Aucto Mk.I with double arms of low strength that allowed for initial experimentation of trajectory control and the early tests of the ergonomic mounting and the direct control of movement.	51
5-4	Earlier iteration of Aucto, showing the safety stops in assembly with the previous version of Joint actuators: double and single MX-106. The shoulder and arm joints are covered with the blue 3d-printed safety stops.	52
5-5	Later iteration of Aucto, showing the safety stops in assembly with the previous version of Joint 2 actuators: double MX-106	53
5-6	Close up of the safety stops of Aucto Mk.II. These safety stops constrain the movement of the joints to a limited range so that the workspace of the SRL never collides with the human wearer, especially the head of the worker.	53
5-7	The shoulder joint of the Aucto SRL	54
5-8	A close up view of a motor joint of Aucto with the carbon fiber tube couplings and the motor joint brackets	54
5-9	The final iteration of Aucto mounted in a testbed to test control systems without mounting to a human wearer	55
5-10	Final iteration of Aucto	56
1-2	Repeated view of the Final Version of Aucto being worn, shown from front and back	57
5-12	Serial Data transmission times, comparing the packet loss difference before and after “clearing” the port.	58
5-13	The 6DOF Optoforce force sensor.	59

5-14	The couplings that mount the force sensor inline with the rest of the Aucto structure	60
5-15	Cross section view of the Granular Jamming Gripper	61
5-16	Bottom view of the Granular Jamming Gripper “cup” and the newly added torque holding feature.	61
5-17	Sealing the Gripper “Head:” epoxy coat curing	62
5-18	Close up view of the gripper with mixed media. The two different media textures, coffee vs. foam beads are visible, as is the separation between the two	62
5-19	The granular jamming gripper. The gripper is comprised of three parts: the head, the cup, and the balloon with media	62
5-20	An example of the way the gripper takes the needed form to hold: a coffee only version of the gripper holds onto the work bench	63
5-21	The granular jamming gripper allows for grasping or holding without the need to aim the gripper in 6DOF. The variety of orientations that can still allow for strong holding benefits Aucto to simplify the system to 3DOF	63
5-22	The pneumatic circuit of the system that powers and controls the granular jamming gripper	65
5-23	A close-up view of the pneumatic valves and circuit as implemented in the Aucto prototype	66
5-24	The handheld control switches that govern the operation of the granular jamming gripper by running the pump and selecting the direction of flow.	66
6-1	SRL Workspace with model of a person and the human arm workspace	68
6-2	The coordinate systems of the gripper	69
6-3	Block Diagram of the control loop	74

6-4	The low level control loop operating inside the Dynamixel Pro motors. This was reverse engineered experimentally to decipher the control loop, so there may be slight differences in the true implementation by Robotis	75
7-1	The Various Tasks: A) Crouching, Supported by SRL instead of own hands, B) Simple Force Holding, Pushing with Force Against Structure only, C) Supporting a Mass at the Gripper for Assisted Tool Holding or Manipulation	80
7-2	Force Measured During a Simple Force Holding Task (Admittance = 0.04m/s/N)Highlighted: small deviations of only a few newtons unless the system is doing fast velocity compensation	83
7-3	Force Measured During The Overhead Compartment Task (Admittance = 0.04m/s/N)	84
7-4	Forces Measured for Various Admittance Values, for the Tuning of the Admittance Parameter	85
7-5	Force and IMU Data During a Force Holding Task	86
7-6	Force Measured During a Tool Supporting Trial (Admittance = 0.04m/s/N)	87
7-7	Force Measured During a Worker Prone Supporting Trial (Admittance = 0.04m/s/N)	87
7-8	Orientation and Position Data During Vector Following Trial; the two angles are complimentary: as θ_1 rotates the shoulder to compensate for the change in Yaw. Shown here is the Yaw angle and negative θ_1 .	88

Chapter 1

Introduction

1.1 Task Motivation, Overhead Assembly in Manufacturing

In the assembly of large commercial aircraft, one of the strenuous tasks are final assembly of fuselage internals, where workers must raise work-pieces and components up to an overhead position and affix them to the ceiling or a wall. These tasks lead to some of the highest number of injuries from long term fatigue and wear, leading to the most time away from work. Upper extremities are the most common injury site, and shoulders are 25% of those injuries. Overexertion and repetitive motion are especially strong contributors to this, with overexertion alone leading to 44 in 10,000 workers being injured annually [1].

The aircraft manufacturing industry is attempting to use exoskeletons, both passive and active, for assisting workers. Passive exoskeletons, including Lockheed-Martin's Fortis gear [3] and Robo-Mate's upper extremity support [4], can balance a heavy load with use of springs and ergonomically designed harness and linkages that distribute the load effectively to the wearer's body. Active upper-extremity exoskeletons have also been developed for lifting supports [5]. These include Cyberdyne's HAL[6], the especially ergonomic designs such as the UCLA 7-DOF arm [8] and the Schiel, van der Helm design [9], and many more that are outlined by Gopura

et al. [7].

While these exoskeletons can augment the human strength in lifting and holding heavy items, the workers at aircraft fuselage assembly must do more than lifting and holding an object. Namely, most tasks require the worker to affix work-pieces and components while holding them at an overhead area. This often requires two workers working together in a confined space: one holding an object and the other securing it with a tool, e.g. Figure 1-1 shows assembly of an overhead compartment requiring two workers.



Figure 1-1: Workers Completing Overhead Tasks in Aircraft Assembly – Snapshot of video of Boeing 787-9 Dreamliner Assembly [2]

Supernumerary Robotic Limbs (SRL) aim to support workers with extra limbs. Unlike exoskeletons, SRLs can take an arbitrary posture independent of the human limbs, opening up new possibilities of assisting the human in close proximity. The SRL attached around the waist can hold an object while the worker is fixing it with

a tool [11][13][12]. The one attached to the chest can support the wearer in taking a crouching posture while working near the floor [14] SRL fingers can assist hemiplegic patients in performing daily chores using an intuitive and implicit control method [15]. A pair of SRL arms on the shoulder has also been developed for assisting a worker in installing ceiling panels [16][17]. An extra robotic arm can even be used to play music and complete rhythmic tasks [21]. These new types of wearable robots are a promising alternative, yet pose new challenges to overcome. SRLs must work effectively with the human in close proximity. Since the robot is attached to the human, the movement of the human may interfere with and disturb the robot [10]. The robot must be lightweight and compact as well as dexterous in holding various objects.

1.2 Overview of Work enclosed

This thesis will then describe herein the design and development of our solution to this problem: Aucto - A novel wearable robot. Subsequent chapters of this thesis divide the work into the following categories:

- Design Concepts - This is a summary of prior work, its influence on this system, and the ultimate design principles and concepts that underpin Aucto's design.
- Human Intent Sensing and Modeling - An overview of the sensing strategies explored and selected over the course of this research
- Human Machine Mounting Interface - A review of the design of the newly introduced exoskeletal suit which interfaces Aucto to the wearer, and acts as the support structure.
- Mechanical Design and Electronics - An extensive review of the electromechanical and structural components of Aucto, from the robot arm, to our implementation and use of the Universal Gripper and pneumatic system and circuitry.

- Controls - The more critical development of this research, the control algorithms and their implementation for force control in a wearable system, allowing for human movement and postural compensation.
- Performance and Results - Testing results of the controls, tuning of parameters and evaluation of Aucto's assistance in manufacturing tasks.
- Conclusion and Discussion

As such, this thesis intends to encompass the complete development of a novel, assistive, wearable robot dubbed Aucto, a shoulder mounted wearable robot arm, as well as the many concepts and prototype investigated over the course of its development.

Aucto, latin for "to augment or to increase greatly", is our supposed next development in human-robot interaction as human augmentation.

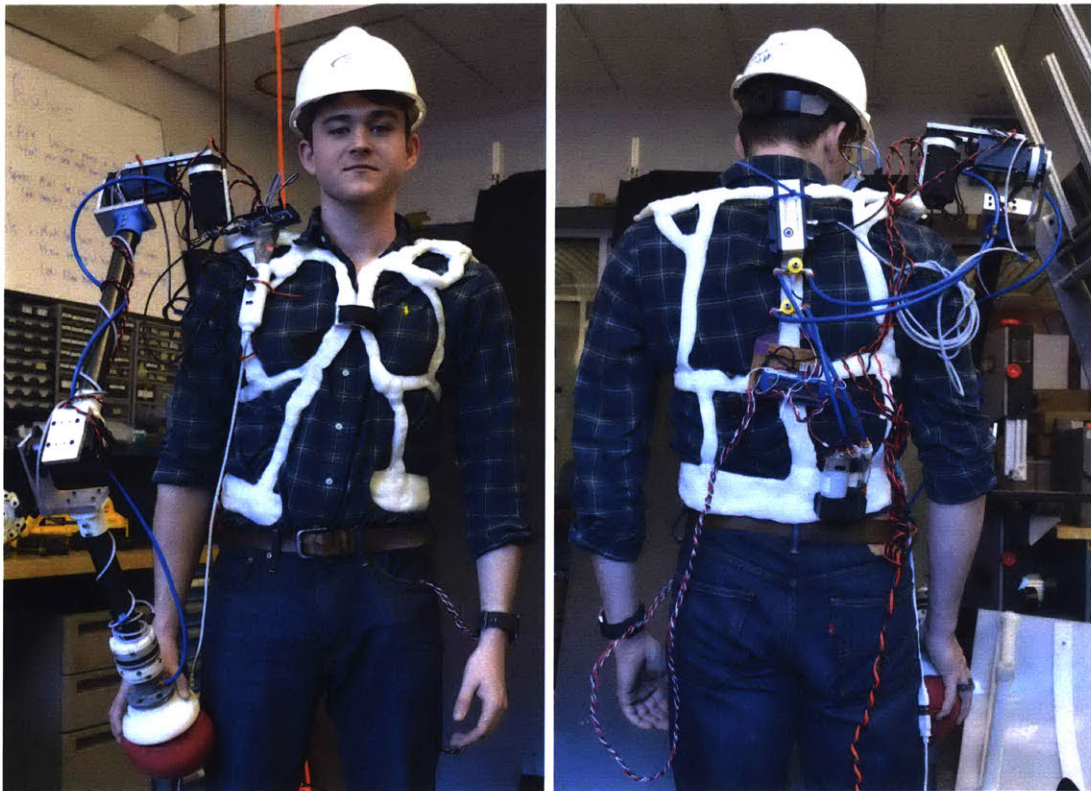


Figure 1-2: Final Version of Aucto being worn, shown from front and back

Chapter 2

Design Concepts

We introduce the fundamental design guidance and reasoning behind the development of the robotic system heretofore referred to as Aucto.

2.1 Guiding Design Principles

Fundamentally, Aucto is intended as an exploratory effort and prototype for a system to be utilized in the work force. As such, the critical features of a robot in the workplace are key to the design philosophy of Aucto.

2.1.1 Safety

In human-robot interaction, safety is among the most paramount concerns to workers. The utilization of robotics in the workforce or in industry principally focus on tasks which are unsafe, tedious, or otherwise "dirty" or undesirable. The use of robotics in manufacturing in many cases applies to all three, but certainly, implementing robotics in the manufacturing line should avoid making it more dangerous, tedious, or difficult.

We play close attention then to the need to increase the safety of workers: reducing fatigue and/or rate of injury to decrease standard risk and designing a robot that cannot hurt the wearer to avoid introducing new risk. The concept of Aucto came from the identification as stated in 1.1 that overhead assembly tasks are risky, inefficient

and taxing.

2.1.2 Flexibility

One core tenant of the work enclosed as well is a focus on the flexibility of the tasks which can be accomplished by Aucto. In manufacturing settings, the need for task-specific programming and maintenance is not only a nuisance, but a costly factor for time and money. Specifically, many workers, mechanics, and technicians are more skilled in programming systems like Programmable Logic Controllers per the industry standard, rather than the languages common to research and academic robotics e.g. ROS, C/C++, Python, etc. Not only this, but the need to re-program a robot for each manufacturing task is a huge limitation to the flexibility of utilizing workers or changing the schedule of the manufacturing line on-line to increase productivity.

Ideally we envision robot augmentation which is intuitive and flexible that workers can utilize in many similar tasks without the need to reprogram the system or have to change internal parameters or calibrate repeatedly. The vision of Aucto is to extend human capability in a way that allows the workers to use the robotic system with similar control input or strategy such that re-training is not needed either.

2.1.3 Ergonomics

Ergonomics and biomechanics of the wearer of Aucto are key considerations given that the goal is to reduce injury and increase capability. Aucto should not limit the wearer excessively to a point where the "cost" of using the system outweighs its benefits. Aucto should be comfortable and leverage the strengths of the human wearer from a biomechanical standpoint. The augmentation should be beyond the capabilities of extra mobile limbs; the extra limbs can feasibly allow for more sensory input that should take into consideration the ergonomics of the wearer.

2.1.4 Simplicity

Simplicity itself lends towards robustness generally, as the fewer components of a system, the fewer points of failure exist. As well, complex and abstract interaction schema typically require more training, more experience, and as well do not lend as easily to the framework of intuitive flexible interactions. We aim then for Aucto to be simple in both the mechanical design sense, and in the sense of human interaction. However, there is no necessity for the underlying controls to be themselves simple; here simplicity of human interaction is to be understood as the simplicity of the input and reaction for a human interaction, that similar inputs yield similar results in a given mode of operation or workspace.

2.2 Wearable Robots

The field of wearable robotics includes a diverse range of interaction devices, exoskeletons, prosthetics and orthotics. This breadth of robotic systems has developed into a rich research field which has multiple inputs in Human-Robotic-Interaction, Sensing, Modeling, Machine Design, Controls and Machine Learning.

One key distinction of wearable robotics is it's close proximity to the human wearer, by definition, but specifically, this yields many strengths in effective assistance, augmentation or collaboration with the wearer. Exoskeletons and orthotics can increase strength, speed, endurance, and rehabilitate or otherwise return mobility to paraplegics and otherwise handicapped users. Wearable interactive devices can be emotional prosthetics, augmentative information devices, interfaces to external devices, services etc. as well as adding new senses to the wearer. There is a new field that is yet burgeoning that is Supernumerary Robotic Limbs.

2.3 Supernumerary Robotic Limbs

SRLs are devices which add extra limbs, fingers, or other manipulators to the wearer. As opposed to exoskeletons which follow or constrain to the human structure and

range of motion, SRLs are an augmentation into a different space. While still young, many interesting interfacing capabilities have been explored that demonstrate the feasibility and advantages of these systems as well as their draw-backs and complexities that differentiate from standard robotic systems. Here we introduce a new contribution to the field in terms of SRL design and controls.

More on the differentiation of SRLs and other wearable robotics is explored throughout.

2.4 Functional Requirements

The current work was motivated by the needs for assisting workers who have to perform assembly tasks in the overhead area for extended time periods. Raising the arms and keeping an overhead position are particularly fatiguing, since the muscle strength decreases as the arm is raised above the shoulder. A viable robotic assist system usable for these tasks must meet the following requirements: Access various sites of manufacturing environment together with an assembly worker; in aircraft manufacturing this requires

- a) moving across a cluttered area, b) climbing a steep staircase, and c) going through a narrow path and moving into a limited space;
- Reach a ceiling or an overhead area, and grasp various objects; in aircraft manufacturing, diverse objects ranging from stringers, frames, and various brackets to plates and boxes must be dealt with; and
- Securely hold an object by pressing it against the ceiling or a fixture in the overhead area.

2.5 SRL for Overhead Tasks

Wearable robots, if designed properly, meet the functional requirements described above. A robot worn by a human worker can be transferred by the wearer, accessing

various manufacturing sites together with the human. If the robot is separated from the worker, it faces hard mobility problems: it must avoid obstacles and go over numerous items scattered on the floor, climb a steep staircase of up to 45 degrees of grade, and move into a small space together with the worker.

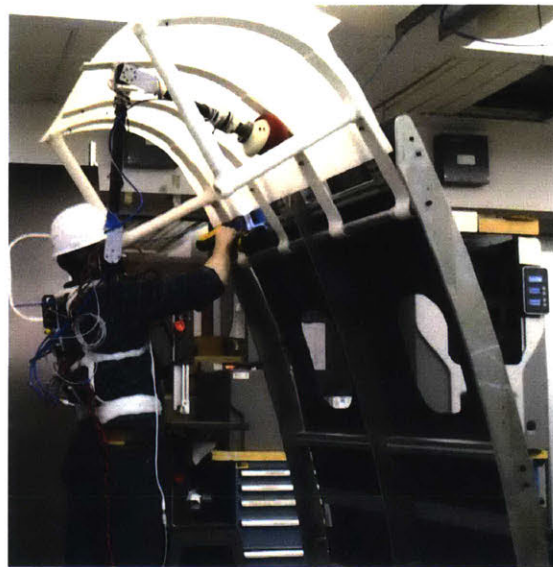


Figure 2-1: A person completing an overhead task with the SRL

The SRL approach can potentially eliminate these mobility and accessibility challenges, and provide a practical solution to using a collaborative robot in a cluttered manufacturing environment, which is difficult to access.

The SRL and specifically the shoulder-mounted SRL should meet other requirements, however. The robot must be lightweight and easy to carry around. Also, the robot must be ergonomically safe and comfortable to wear. Not only the gravity force of the robot but also the forces acting on the robot are both loads to be borne by the human. Not merely the robot must be made lightweight, but its interface with the human body must be designed carefully, so that the loads can be distributed effectively to the entire body. As will be discussed later in the implementation section, a) the kinematic structure of the robot must be designed for safety as well as for meeting the workspace requirement, and b) a robot-mounting gear that can effectively distribute the loads and transmit them to ground will be designed. Furthermore, the robot will

be made lightweight by reducing the number of powered joints and using lightweight materials such as carbon fiber links and aluminum support brackets. The Granular Jamming Gripper described below is effective for reducing the number of joints as well as for grasping various objects.

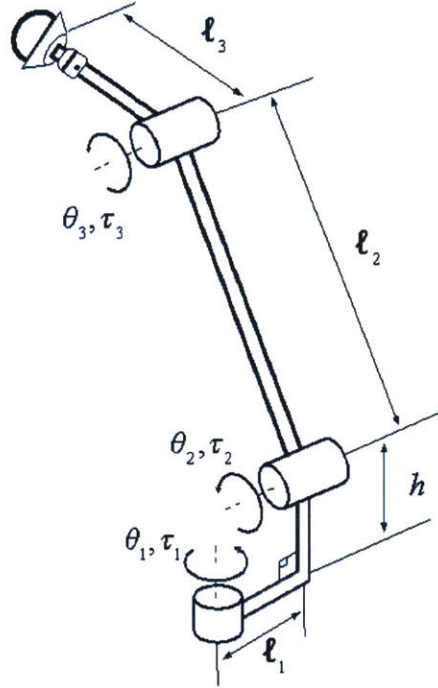


Figure 2-2: SRL Kinematic Structure

2.6 Use of a Granular Jamming Gripper

To make the robot lightweight and simple to operate, we need to minimize the number of DOF. However, this poses the problem that the arm must be able to grasp objects of various dimensions and shapes and from different angles or postures of the robot. This has been accomplished with many versatile gripping strategies and types of grippers, ranging from under-actuated grippers to modular to biomimetic grippers [25, 26, 27, 28, 29, 30, 31] however, in each of these cases the gripper is to be mounted on a high DOF arm that can position the gripper in 6 DOF to allow for the correct

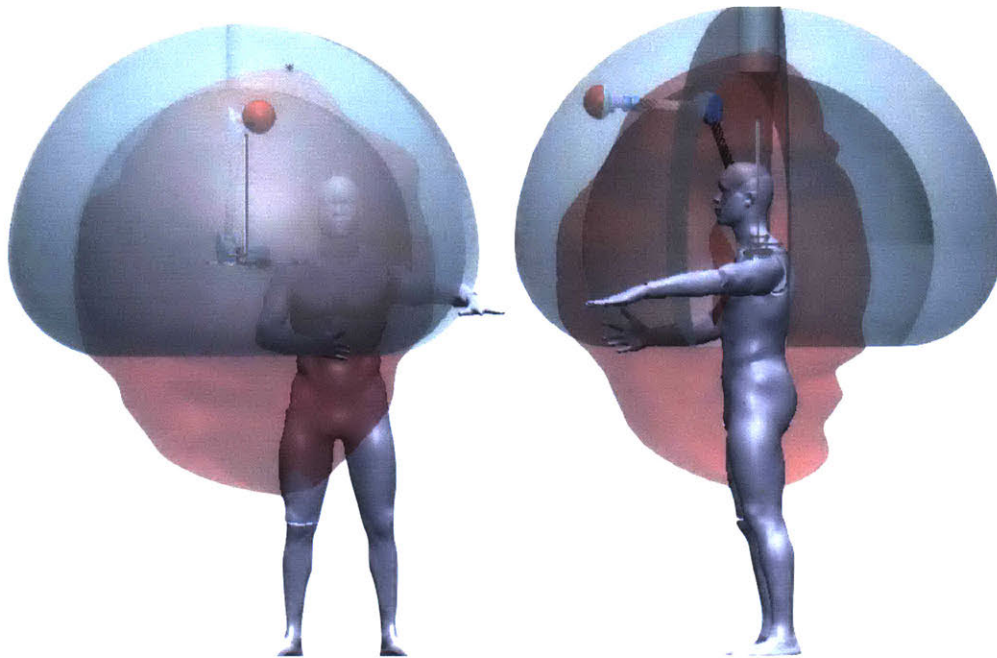


Figure 2-3: SRL Workspace with model of a person and the human arm workspace

grasping posture. We elicit the use of the universal granular jamming gripper as proposed in [25, 26]. Since the gripper not only adapts to any part geometry semi-passively, it can harden to shape without needing complex orientation. See Figure 2-4 Effectively, the end effector only needs to be pressed against the object and it can harden to grasp and support the object.

For this specific application, we also note other advantages not otherwise explored in other literature involving granular jamming grippers:

- The jamming material is strongest under compression which is the typical use case in our supporting task
- By dynamically changing the internal pressure of the gripper, the jamming media can be treated as a stiff, highly damped fluid rather than a solid, fully-jammed media
- New design features of the gripper structure allow for increased force transmission in tension and in rotational shear

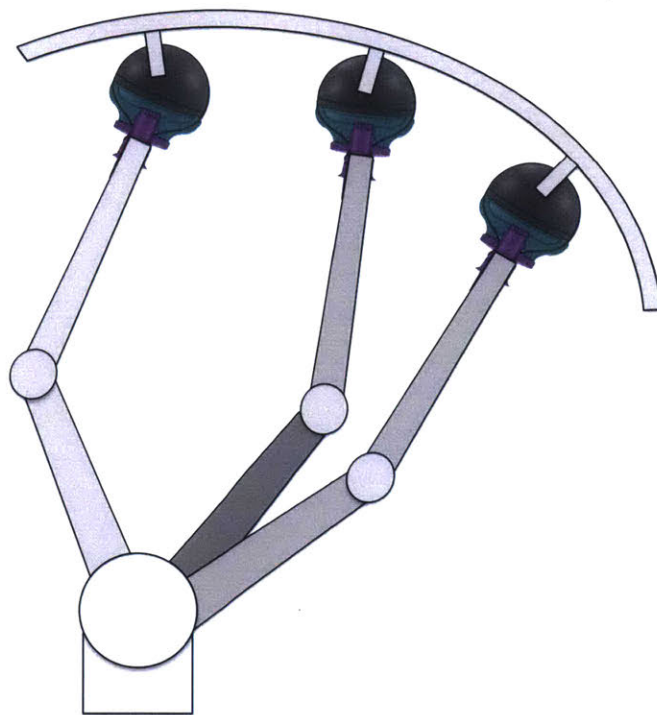


Figure 2-4: Granular Jamming Gripper can grasp objects from an arbitrary direction, eliminating the need for a powered wrist

Chapter 3

Human Intent Sensing and Modeling

An initial goal of this project was to specifically be able to accurately model the tasks being completed by the worker, and to follow the commands based on the context of the work, or rather to be able to even anticipate the motions of the worker to assist, avoid, or interact in the context of the manufacturing tasks. Several strategies were examined at a high level, and from this breadth of research, the simplicity of Aucto eventually arose. However, it is clear that many of these strategies are possibly highly effective given deeper treatment.

In a gross simplification, there are two key forms of this sensing and modeling strategy explored herein: collaborative and human augmentative (via implicit or explicit control). In this limited definition of collaborative, the robot and the human have distinct tasks to complete, and as the human completes their tasks, the robot completes the collaborative tasks in parallel. The human and the robot are separate in their planning but share a model of what tasks each should be working on, they are partners in completing the task. In contrast, the augmentative approach treats the tasks space more fluidly and any task can be completed by worker or machine. In fact it is the human's decision and commands that would drive the robot to work or even in some cases, the robot is under direct control from the human worker.

In the case of a collaborative strategy, the robot and human begin to work fairly

independently, the robot has some model of the tasks to be completed and that model extends to the human worker. The robot can wait for the human to complete a task before moving on; it can work on the set-up of the next or gather a tool that the worker needs as the progress moves forward.

To take the example of our earlier described task of mounting an overhead compartment while assembling a plane:

The robot will pick up the panel with the human when they approach it as this is the first task, then while the human holds one side, the robot can get the socket driver and hand it over to the human and begin to hold up the full load of the overhead compartment as the technician fastens it in place. The robot may be using a suite of sensors, monitoring motion with IMU, the tools in hand via RFID/NFC or computer vision, position and posture via IMUs or object recognition or many of the other varied strategies employed in the varied examples in contemporary collaborative robotics. The robot's model of the world or tasks may be statistically driven or may be a fixed set of confirmed instructions coupled with the interaction with the human. Either way, the idea here is that the human does not need to control the robot per se. They are two partners with a very different interaction than two human workers. Because of the collocation of the robot worn on the human, the human has direct haptic input as to what the robot is doing without needing to watch, communicate or otherwise interact with the robot.

In the case of the augmentative approach, the key focus is more on extending the one human to have the capability of two rather than having a partner. The wearer of the SRL could directly or indirectly control the motion/force/velocity/effort of the robotic limbs more like they would move their arms. Rather than commanding tasks through signals, or letting the robot make decisions on the task to complete, the human can more flexibly treat the SRL as a tool that extends their performance rather than couple or partner the effort.

In the case of the overhead compartment task:

The worker approaches the panel where it is stored and commands the arms to pick up the panel. This may be done through direct commands or signally, or maybe it is

followed through implicit commands that the robot knows to follow certain motions of the worker's arms and grabs the object as the worker grabs it. The worker progresses through the task but uses redundant degrees of freedom to signal the robot to follow or complete motions, this can be through eye gestures, through head movement, moving the arms in a certain way while still working on the task at hand; there are many possibilities.

Another valid categorization of these two is commanding tasks for the robot or commanding motion. There are pros and cons to each, and we explored some different embodiments of each.

3.1 Sensing Human Task Execution and Intent

A principle problem to address is to allow for the SRL to sense the motion or task execution of the worker, or even more deeply to sense the intention of the wearer. In most applications, the intent cannot be measured directly, rather the models allow for intent recognition, but in some cases, such as eyetracking or gesture/command recognition, complex models that contextualize the motion are not needed. For the latter cases, we treat this as sensed intent to draw a distinction between sensing vs. modeling for the sake of exposition.

3.1.1 Sensing Motion

Earlier iterations of shoulder-mounted SRLs used Pololu MiniIMU-9 v2 IMUs which were 9DOF (3-axis for accelerometer, gyros, and magnetometer). Three sensors were used: one on the head, one on each wrist. This was used for human motion classification.

In the newest concept investigated, a sensor suit was designed to house 13 IMUs in the configuration shown in 3-2. More on the exact use case to be explained further below. The sensors selected for this system are the BNO055 sensors in the Adafruit breakout package.

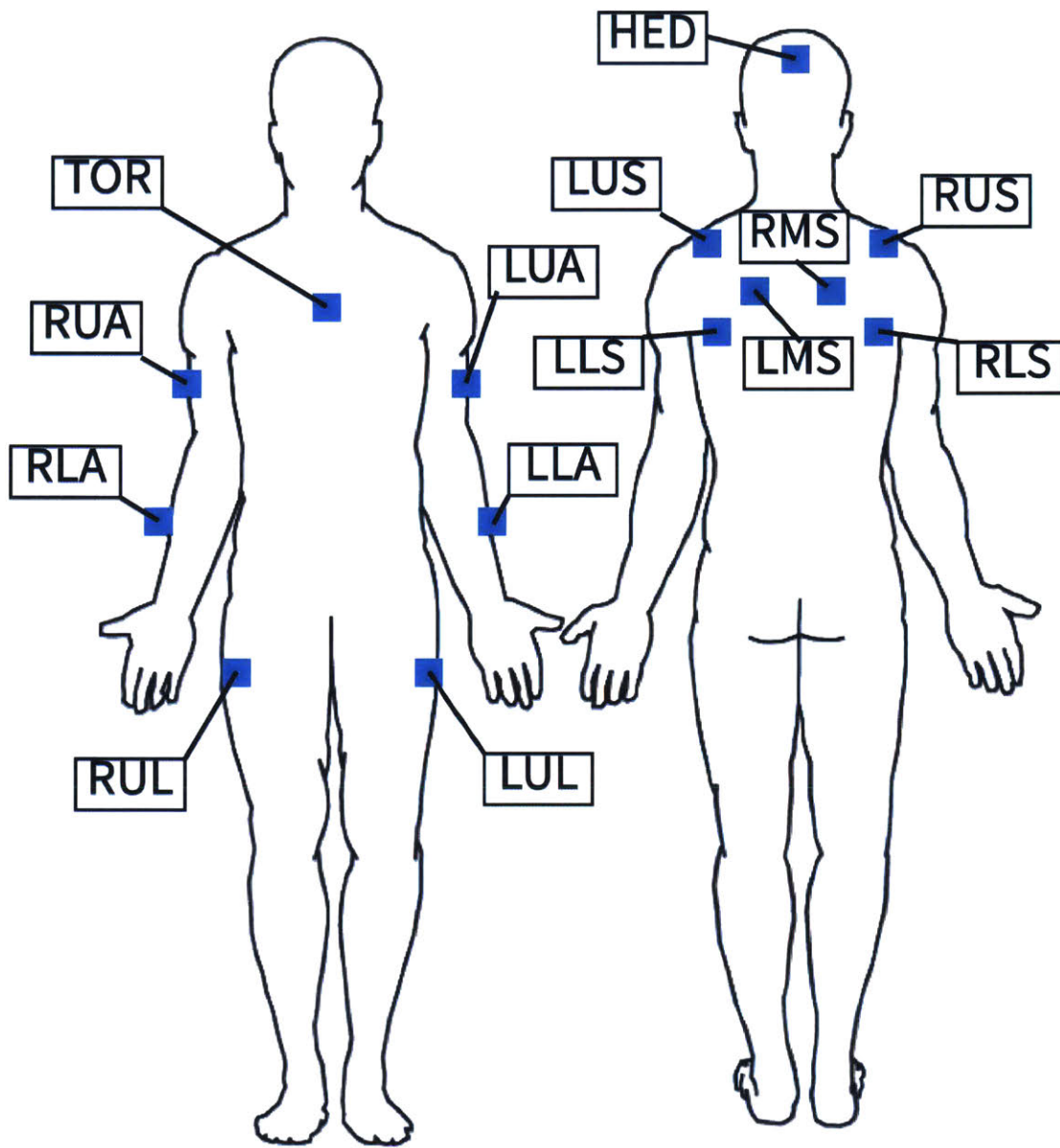


Figure 3-1: Mounting locations of all the IMUs in the sensor suit concept

3.1.2 Sensing Posture and Orientation

Critical to worn robotics is the compensation for human motion. Accelerometers and gyros can be integrated over time to give changes in position in 6DOF, but these signal are noisy and prone to error especially in x-y-z where the signal must be twice integrated to get a position measurement. However, 9DOF sensors have an additional measure of the magnetometer to give more accurate measurements when coupled with

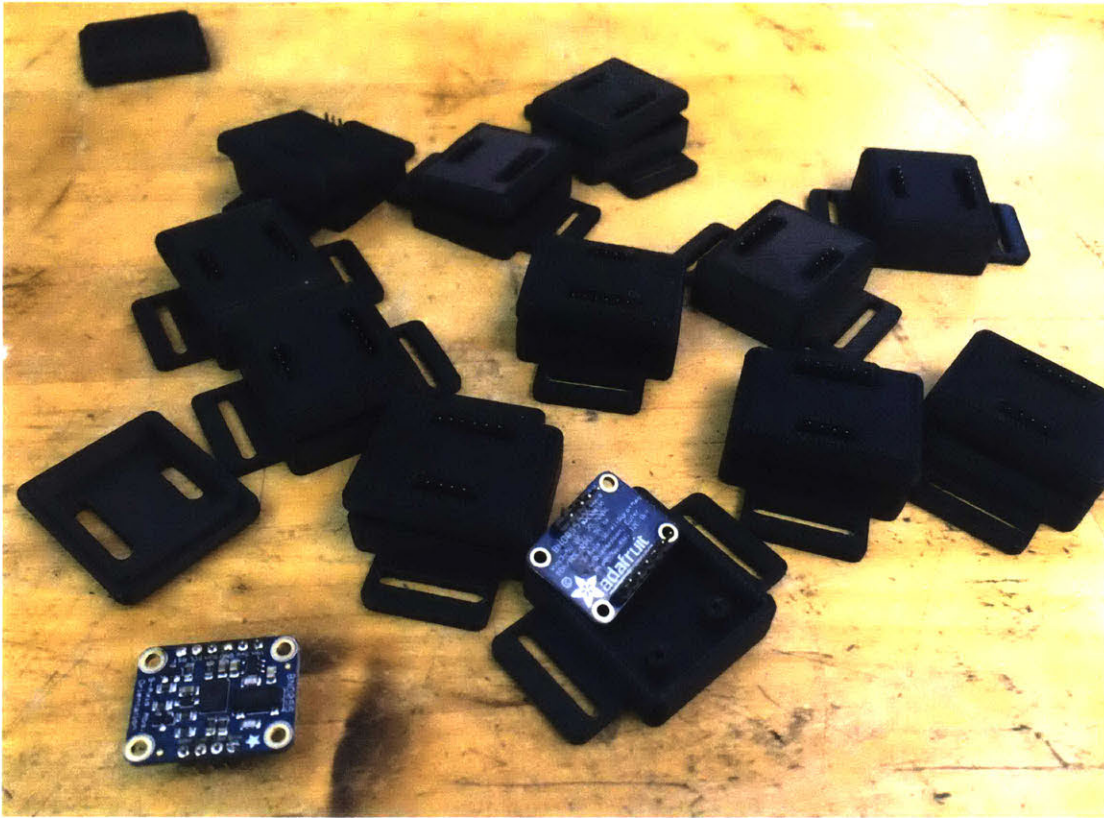


Figure 3-2: BNO055 sensor packages inside custom cases which allow attachment via strap, adhesive, sewing, and other methods, though this is what had been employed.

sensor fusion.

Additionally, being able to track orientation of the various sensors is critical to modeling the human worker as limb position or orientation is much more important to the safe operation of the robot than instantaneous movement.

Looking towards off the shelf solutions, the researcher selected the BNO055 sensor package which uses Bosch's on-chip sensor fusion to track the orientation of the board in space. The 9DOF sensor has 16 bit gyros, 14 bit accelerometer, and a magnetometer with $\pm 2.5^\circ$ accuracy. The sensor package is capable of outputting data at reasonably high rates: 1000Hz for Acc. data, 523Hz gyro, 30Hz mag, and the data fusion output of 100Hz. This data fusion algorithm allows for tracking of absolute orientation as quaternion which allows robust manipulation of our coordinate systems and simple, fast computations of changing coordinate systems.

The sensing of the orientation of the sensor is key to being able to compensate for moving coordinate systems. In the case of the SRL, the human wearer may lean, turn, twist, and all of this motion is needed to complete the tasks at hand. This inevitably changes the coordinate system of the robot as its base if the human wearer. Many compensation techniques have been investigated in applications ranging from robotics on vehicles or specifically non-inertial systems like ships and sea-based platforms that undulate with the waves, in wheelchair based systems for assistive robotics, or in multi-robotic systems in the example of the macro-mini manipulator robotic designs.

See Chapter 6 Section 3 for deeper explanation of the final embodiment of our compensation algorithms. Eventually, the final use of these orientation sensors was simplified to one sensor at the base and more of the motion compensation was accomplished by the admittance control developed.

3.1.3 Sensing Intent and Focus with Eyetracking

Another effort to expand the sensing suite of the SRL project was to incorporate eyetracking to allow for the SRL to measure the focus of the wearer or for the wearer to communicate intent with their focus. The eyetracking was done with a modified consumer HD webcam. This webcam was disected, the illuminating LEDs were swapped out with IR LEDs and the IR filter removed from the camera. The LEDs were driven at low intensity to avoid serious affect to the wearers eye which is critical given that IR light does not trigger the human avoidance/blinking reflex. However, this does allow for the tracking to be completed in various levels of lighting without much calibration or environmental dependence.

The algorithm to track the pixel coordinates of the pupil is as follows:

1. blur image for noise reduction
2. normalize to grayscale
3. binary threshold the image based off of the minimum values of reflected light received

4. invert the image
5. find object contours using the border following edge detection algorithm implemented in OpenCV from Suzuki et al. [35]
6. calculate the areas, centers and circularity of the contours detected
7. select for objects with areas and circularities with the desired range
8. sort objects by distance from previously measured pupil location, select nearest object
9. fit an ellipse to this object
10. return the center location of the best fit ellipse
11. if no object meets the selection criteria or is unreasonably far from the previous measured location, it is rejected and the value from the previous video frame persists

In order to get useful measures of the direction the wearer is looking we convert these pixel dimensions to angular coordinates, giving a vector to project from the eye to the object for useful interpretation. To do this we initially calibrate the sensor by getting a measure of the range of motion of the eye (have the wearer look maximally up/down/left/right) and mapping these values to the maximal values for the azimuth, ϕ , and the elevation, θ , as well as the pixel coordinates of the center pose, calibrated by having the wearer look straight ahead. Using these data, we can approximate the radius of the eyeball to be used for the mapping of the 2D image to the spherical coordinates. Then, as we capture pixel coordinates from the eyetracker, the deviation from center and the following trigonometric relationships are used to calculate the angular position of the pupil in terms of elevation and azimuth.

$$\phi = \arcsin \frac{\Delta x}{\sqrt{R_p^2 - \Delta y^2}}$$

$$\theta = \arcsin \frac{\Delta y}{R_p}$$

From these spherical coordinates we can understand where the person is looking. The SRL can be commanded to move in this direction or perhaps given more knowledge or instrumentation of the environment, the object the wearer is looking at can be derived and the SRL can be commanded to grasp or manipulate it. In part of our exploration for direct control, it was initially explored but not fully implemented that signals could be interpreted from looking in certain directions and shaking the head. The head shake was sensed with a head mounted IMU, using a lightweight classifier that looked for a frequency band of oscillation lasting for a specific window of time. While this was never fully integrated with Aucto, similar techniques were originally explored by Baldin Llorens. [16][17][19][18]

Experimental tracking of the human eye showed that the recognition rate was not impacted significantly by the external lighting environment thanks to the IR illumination. The use of selecting nearest neighbor objects and rejecting objects that do not match the size and shape criteria make the algorithm robust to rapid eye movements, poor or odd reflections on the cornea, common eye tracking issues such as recognition against eyelashes, blinking rejection or other false positives.

A video of the eyetracker in action can be found at:

https://youtu.be/-NR7_d8kFsc

3.2 Task Modeling

As earlier described, one of the possible control strategies explored was to leverage the structured nature of manufacturing to control Aucto with a sequence of defined tasks, to be completed in parallel or in tandem with the human wearer as he/she completes the tasks. In order to do tasks collaboratively with the worker, Aucto must be able to model the task and the state of the worker/tools/task completion status.

3.2.1 Colored Petri Nets

We expand on the work primarily begun by Llorens et al. [19] to use Colored Petri Nets (CPNs) to model procedural tasks that have multiple agents and tools to be used. In previous work and existing software, CPNs are compiled from the network model into a representative binary tree or set of if/else statements about sensed measurements or task sequences. This was done to confidently avoid collisions or states that could be in conflict as the CPN software evaluates the ambiguity to confirm that there is only one possible state given a set of measurable conditions. For example see Figure 3-3. Here, it is evident that in prior work, the state machine can only be linear i.e. you can only progress forward or stay in the current state. This makes logical sense for any given set of tasks, however, we have the problem that certain tasks are not so explicitly ordered. The system may branch off, return, or divide tasks up.

As a result, a new network generating software was developed with the assistance of an undergraduate researcher. The beginnings of this software are to allow for complex graphs to be designed, as well as generate classes for actors and tools which can traverse these graphs to allow for another modeling procedure to evaluate the status of the system or manage the status of an actor or tool. Future work can expand on this software to generate more more intuitive interface like that of the CPN tools software used in previous work.

3.3 Statistical Modeling

The next step is then to be able to inform this model with sensor data and a statistical understanding of how the graph of the CPN should be traversed. We explore the use of Partially Observable Markov Decision Processes (POMDPs) as a way to map sensor signals to real states and leverage the existing graph structure of the CPN as a mapping of the POMDP graph.

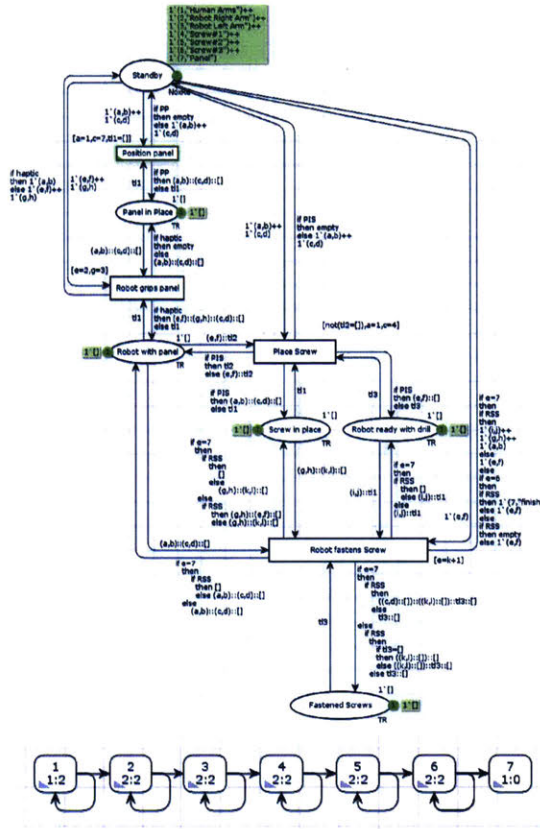


Figure 3-3: Colored Petri Net Model developed by Llorens et. al [19], shown is as well the compiled state machine of the CPN.

3.3.1 POMDP Models

POMDP models are essentially statistical state machines coupled with complex solvers that resolve the current state based on the current observations. There are several levels to the graph: hidden states, beliefs, observations, actions, and rewards. The possible states, and their mappings from action and corresponding observations exist a priori and during execution, the robot measures the sensor signals to yield observations, calculates the most likely state and takes the action which has the highest expected value for returned reward. We use the CPN as the base level of the possible states and transitions based on actions, as the actions are the state transitions. We structure the rewards as a measure of progressing the task forward, with negative rewards or penalties for failure or interference in the human actions.

The success or failure of a task is measured with a combination of inputs: successful completion of an action by the SRL, and human feedback in the form of verbal or gestural feedback. For example, if the robot does something incorrectly, the human interrupts and informs via gesture that the robot should stop. This heuristic allows for the robot to as well get another observation to assess the state.

3.3.2 POMDP Software

The initial mapping of sensors to observations is completed with a feature recognition classifier, e.g. a Support Vector Machine, neural network, or K nearest neighbors classifier for example. The data collection process requires an initial ground truth which has hand labeled data. Then the sensor suit designed for Aucto takes in complex data and we then can compare the running data to the model created by the classifier trained on this ground truth data. As well, this same data allows for the probabilities of transitions given an observation as enough data must be collected to give a reasonable figure for all possible transitions, any transitions not measured are seeded with low, non-zero probabilities.

The development of the task graph modeling software allows for the same model structure to be output as networks that seed the POMDP model. The only additional computations and elements to be added are the mappings of the actions, observations and rewards which are taken from the data model computed from observation data.

3.4 Control from Redundant Degrees of Freedom

The concept is that the human arm has many degrees of freedom, and with the shoulder of the arm included, this amounts to 10-14 DOF thanks to the amount of movement the scapula can make along and around the back/shoulder, and that the shoulder can move w.r.t. the clavicle and the clavicle w.r.t. the sternum/torso. However, a rough motion analysis completed by Pan G. et al [23], shows that the shoulder joint alone has 10DOF rather than the traditional 3DOF proposed commonly in literature. This would then yield a 14DOF system. We propose that these redundant

DOF can be used as control input to the SRL. In the standard formulations of literature the arm is cited at having 7 DOF; this calculation typically assumes only the 3DOF of the glenohumeral joint. It is the addition of the aforementioned degrees of freedom of the scapulothoracic , acromioclavicular joint, and the sternoclavicular joint that we can have additional modes of input to the SRL. It is notable that these models do not include the many redundant DOF of the human hand, which adds many more DOF.

We suggest then to leverage the redundant DOF of the human arm/shoulder as control input. The human wearer can complete movements or manufacturing tasks while manipulating the shoulder, compensating for the motion of the shoulder is qualitatively simple given that the movements in these DOF are both redundant and independent of the other DOF needed to manipulate in 6DOF.

Various control schemes can be implemented to include this direct control e.g. the “shrug” of the scapular elevation can be interpreted as signal for the SRL to move upward, adduction can signal the SRL to move laterally while abduction would move the SRL medially. These types of movements replicate and amplify the motions of the natural limb and while the wearer compensates the motions out in said natural limbs, the SRL can be manipulated.

The concept proposed in this research is that 3 DOF manipulation in XYZ translating coordinates is possible by leveraging these redundant DOF.

This concept was initially tested by embedding switches used as direct input that would command a motion along a trajectory when pressed. The switches were all along the exoskeletal human-machine mounting and could be pressed by moving the shoulder around. The extra mobility of the shoulder allowed for the wearer to press the buttons only when they wanted to and could otherwise complete tasks without pressing the buttons. We advise that in future reserach that quantitative analysis of this be further explored to provably demonstrate the effects on human motion control. This switch based implementation was especially limited as the switches were difficult to actuate and would occasionally be outside the local workspace of the human shoulder do to singular configurations of the shoulder itself.

3.4.1 Neural Network Sensor Suit Concept - Redundant Shoulder Control

We return the the sensor suit shown in 3-2. This wide array of sensors is meant to allow for very precise measurement of the motions of the shoulder while also being able to capture the pose and motion of the arms, torso and lower body. This specific configuration is for a proposed direct control of the SRL using the above proposed Redundant Shoulder Control. The use of the mechanical switches obviated the problem that the range of motion of the shoulders in these DOF is difficult to measure precisely and more control than On/Off was needed to complete tasks.

The concept of using machine learning classifiers then to recognize the shoulder motion would allow for much more complex input where intensity and speed or the motion could be classified into vectors as well as recognize synergized motions moving in more than one DOF at a time.

To experiment with this concept we begin with a reimplementaion of the recognition task completed by Ordóñez et al [33]. They use a Deep Convolutional and Recurrent Long/Short-Term Neural Network to do feature recognition on the Opportunity Dataset [34]. This DeepConvLSTM network as they call it was reimplemented and the data restructured to match the IMUs that we will envisioned for use. This included modifying the original resolution of the Opportunity datasets sensors as well as changing which channels were used in classification. The initial tests found that the very unbalanced input dataset was very difficult to train and therefore much post processing was needed to get an accurate output. However, the published results of Ordez et al suggest that maybe insufficient training time or differing techniques/-training parameters may be to blame, as variance in the dataset used may greatly effect the influence of the parameters to be used.

Despite some pitfalls the classifier still managed an F1 score of .97, falling just a bit short of the DeepConvLSTM data with much less data to classify on. The next steps in this research are to build and test this sensor suit fully to allow for the classifier to be applied to the SRLs.

3.5 Sensing Human Fatigue and Human Fatigue Modeling

In addition, we posit that one of the key contributions that wearable robots like Aucto may be able to produce is in fatigue monitoring and understanding the state of the human worker in the sense of productive work capability, probability of fatigue, or changing interaction strategies to match the fitness of or strain on the technician or operator wearing Aucto.

Chapter 4

Human-Machine Mounting Interface

One of the critical design considerations for wearable robotics and more specifically in worn robotic limbs is the way load is transferred into the human wearer and how the robotic limbs are attached to the body. Comfort is very key and the transfer of load should be directed through strong parts of the body without causing pain or other discomfort. As well, we have brought into consideration the concept of haptic feedback that can be effectively proprioceptive for the wearer.

4.1 Worn Robot Mounting

Traditional exoskeletal design has many of the same design constraints and therefore is useful reference. These systems typically are designed to interface comfortably and use a continuous structural loop as shown in 4-2 which allows supported loads to transfer directly through the structure of the robot from end effector down to the earth. Many of these systems are rigid, lightweight, and stiff to allow for comfortable and sturdy practical use.

Sometimes referred to as series exoskeletal structures or in some cases prosthetics and orthotics, many worn robotic systems have been formulated to interface with and enhance the human body.

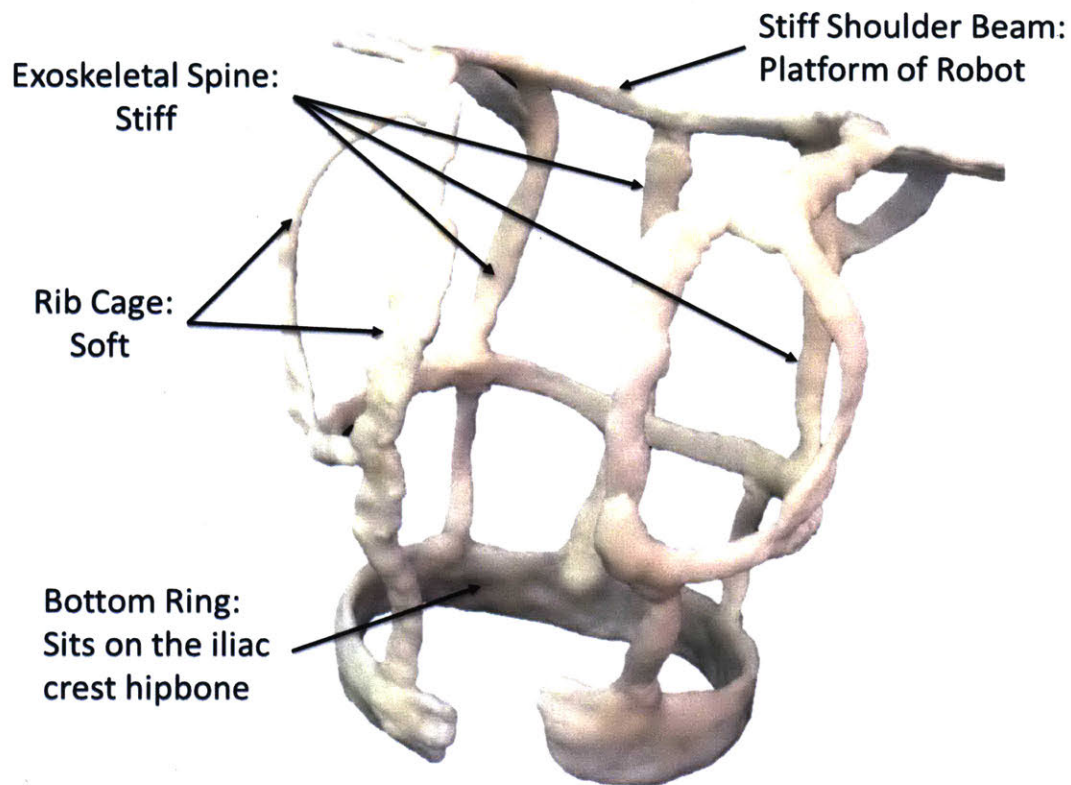


Figure 4-1: Prototype of the Ergonomic body attachment or "ExoSuit"

Prosthetics namely [20], have shown that there are optimally comfortable interfaces that take into account the hardness of the human body or where the robot is interfacing. As well, some systems have been designed to have a varying stiffness that transitions from soft to stiff to better interface with the human body and prevent uncomfortable pressure. All the while, these systems allow for the distribution of load across the human body, rather than apply at distinct points.

Other existing SRL devices have been mounted with vests[14], hiking equipment and harnesses[12, 11], custom rigid mounts[19, 16, 18][10], as well as gloves and items sewn into clothes[15]. Many of these devices share a trend of rigid base supports holding the robotic elements and use a cushion of padding, cloth rubber or other softer element between the human and rigid frame to soften the attachment.

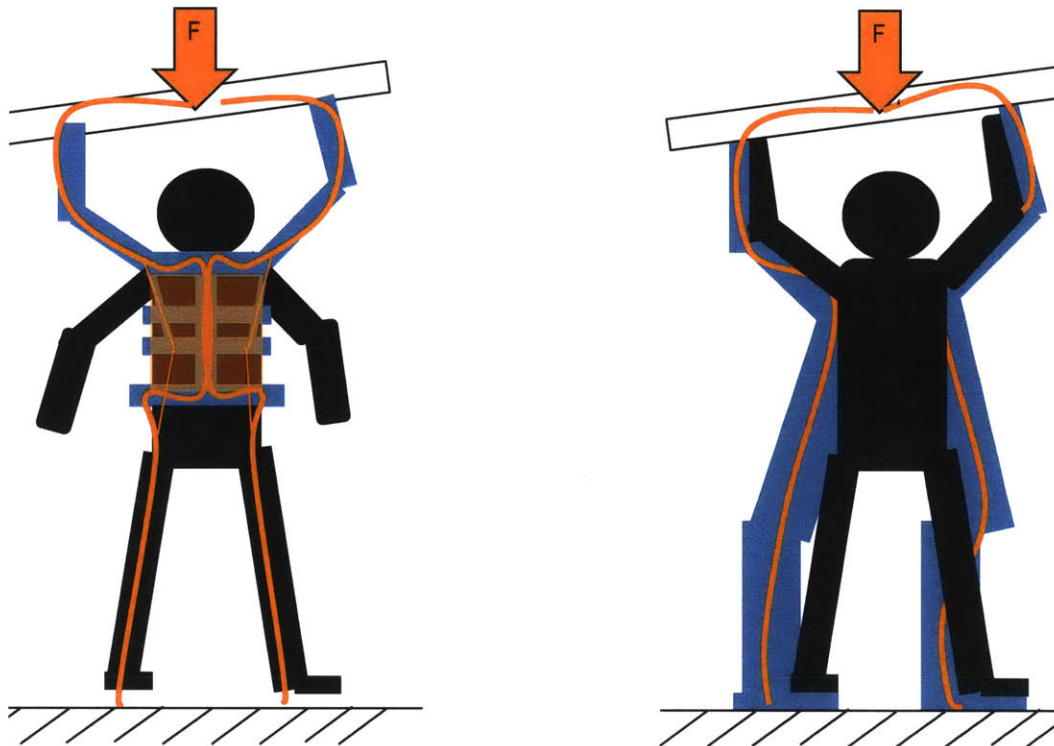


Figure 4-2: The structural loop of the new ergonomic attachment vs. a standard exoskeleton or person

4.2 ExoSuit Concept

We introduce a new design. This core concept is to have a stiff structure that transmits the majority of the loads to the iliac crest of the hipbone. There is a stiff platform that supports the robotic limb base joint, this is connected to an exoskeletal “spine” that is made to be very stiff in axial load, bending, and torsion. The spine is connected to a hip structure that can then transfer loads to the wearer. In addition to this simple, stiff, base structure, there is another structure of less stiff components.

We model this concept based off of the human rib cage to an extent, where the loads are by majority borne by the spine, but forces can be distributed across the torso to increase stiffness and reduce load on individual points along the spine.

From this concept we develop the structure shown in 4-1. which points out the

thin members that act as the sternum and ribs of the design. These pieces of the structure are oversized in comparison to the wearer and tension is applied to compress the exoskeletal structure onto the body. The internal stresses here make the structure stiffer, and the compliance of the thermoplastic make this suit versatile to many body shapes and morphologies. This structure then distributes some of the torsional and axial loads over the torso, but the structure is to be very compliant such that the majority of load is borne by the spine. This is accomplished by ensuring stiffness of the supporting base at the shoulder and designing it such that little strain occurs here.

A key concept that makes this exoskeletal structure novel is the way the loads are distributed across the torso. We design the thin “rib” members such that they buckle under small deflections, pushing into the torso with even small strain at the robot base. This amplifies the strain, but transmits little load to the torso, allowing the wearer to have sensitivity to the forces applied by the robotic limbs while having little pressure or load borne on soft tissues, avoiding discomfort. For different loads and directions of loading, the members will apply slightly different pressures across the torso, yielding a mode of proprioception that is not present in traditional worn robotics. Figure 4-2 shows the structural loop that the loads traverse as well as the force transmitted member to member.

4.2.1 Comparing to Other Systems

The main differentiators of this mounting system is its focus on proprioception and flexible load redistribution.

In contrast to exoskeletal systems, our system does not avoid the wearer bearing load. Rather, this load is transferred to the wearer by design to allow for proprioception, as well as taking cues from some exoskeletal systems that direct loads to the hips and lower train that can have the most strength of the human wearer typically. As well, the elasticity of the load bearing elements is meant to allow comfort without much soft padding, whereas many prosthetics, orthotics, exoskeletons and even other SRLs in literature have needed the padding to avoid irritation of the skin, bone, and

tissue.

In contrast to many other worn systems, we do not rigidly constrain the base as in [16, 12, 5, 6, 8] and many many other designs. The flexible base is part of the proprioceptive design, and so the robotic base may be stiff, but because we measure the orientation of this base in real time (see Section 3 and 6 for more detail) this does not effect the control scheme, and may add to comfort as pointed out in Pan G. et al. [23] because it avoids constraining the wearer joints. Of course, this means that the system is inherently not stiff. This is both a positive and negative: in the case of our admittance controller, this allows us to be significantly more stable by introducing additional low-stiffness members into the system to avoid the instability of the controller in contact with stiff systems, however, this adds in more dynamics to the system that the controls must be robust to, and other resonant modes to avoid.

As well, we envision that this system is fairly flexible to variations in body dimensions. While designed for average proportions of the typically adult male workforce of the aircraft industry (conveniently fitting the investigator), the system was built with an adjustable buckle/strap that pulls the structure in tighter, while the flexibility of the structure allows it to open up. We estimate that it can fit a range of waist sizes from 26-36" measured just above the hip, not necessarily in line with the wearers pant size. Currently, the ratio of hip to shoulder dimensions, as well as the placing of the flexible rib members, assume the broad shoulders and flat chest of a male wearer, which we recognize could be easily iterated to better fit female dimensions, but this was not in the scope of the enclosed work.

4.2.2 Fabrication

For the purposes of making the suit iteratively and with tunable properties, we elect to use lightweight thermoform plastic that can be hand molded, known as InstaMorph. The material comes in pellets, is melted into thermoplastic state with a heat gun as shown in Figure 4-5, and then, molded by hand into different smaller parts. These smaller beams can be fused together by melting two ends of separate joints and forcing them together so that they cool into one hard piece. Initial versions of the ExoSuit

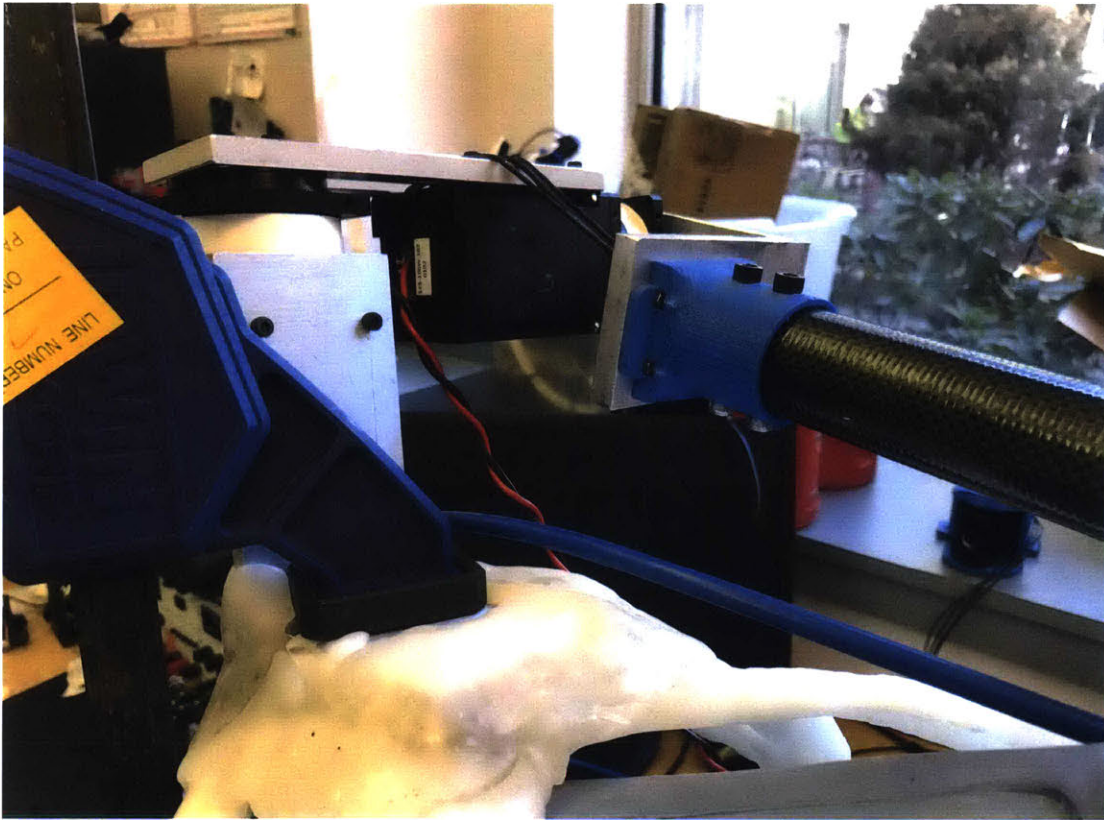


Figure 4-3: The base of the SRL is insert molded into the stiff shoulder platform of the ExoSuit

were molded around the form of a dummy, then shaped to the rough size of the wearer.

The thermoplastic also allows for the embedding of objects into the suit much like over-molding. A strap is embedded to allow for tightening of the system to introduce the internal stresses and increase stiffness, as well as allowing for a variable size for the suit. And as shown in Figure 4-3 the base motor bracket of Aucto is mounted directly by embedding it inside the shoulder of the ExoSuit.

4.2.3 Testing and Iterating

Qualitative tests on comfort, fit, and the ability to sense the forces loaded allowed the wearer to identify pinch points, areas that were too stiff or too soft, and be able to mold the geometry iteratively to fix this. Using rapid prototyping thermoplastic



Figure 4-4: Instamorph of the ExoSuit cooling; transparent when plastic, opaque when set as "glass"



Figure 4-5: The Process of heating the instamorph to prepare it for molding: heating until thermoplastic

allowed for quick adjustment and organic reshaping of the model as needed.

We completed proprioceptive tests qualitatively as well, with the wearer identifying the direction of force applied while they are blindfolded. The data collected here is not significant in volume or depth to publish, however, future work can collect



Figure 4-6: Tennis Ball Mounting used in the intial proprioception trials

more conclusive data on the matter. Figure 4-6 shows the equipment used for the trials was simple: padded, stiff arms were mounted to the base and an assistant can apply force while the wearer is blindfolded.

Chapter 5

Mechanical Design and Electronics

5.1 Robotic Arm Design

5.1.1 Kinematic Structure

Thanks to the Granular Jamming gripper, the number of degrees of freedom required for the arm reduced to 3. This not only makes the robot design lightweight and compact, but can make it simpler to assure safety than for a full 6-DOF robot. The work space can be determined in a straightforward manner, and potential interferences with the human body, in particular, with the face can be evaluated without difficulty. Figure 2-2 shows the kinematic structure of the 3-DOF arm. The horizontal offset l and the vertical offset h at the first joint is for avoiding interference with the face.

Figure 2-3 also shows the workspace of the prototype robot. The link lengths were optimized to be slightly longer than standard human reach and keep the workspace volume large yet distant from the worker's head and arms. Joint stops are used to prevent the workspace from extending into the human body. The key joint stop is that of the base joint, joint 1. As shown in Figure 2-3, the head is kept outside of the volume of robotic workspace and the arm's end effector cannot reach to a point above the head of the wearer.

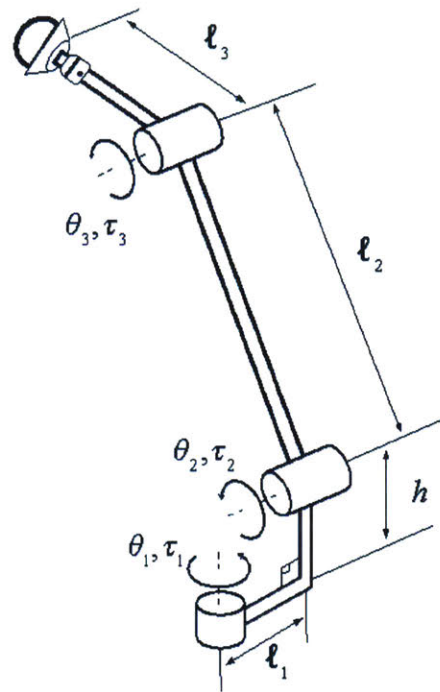


Figure 2-2: SRL Kinematic Structure, repeated for reference

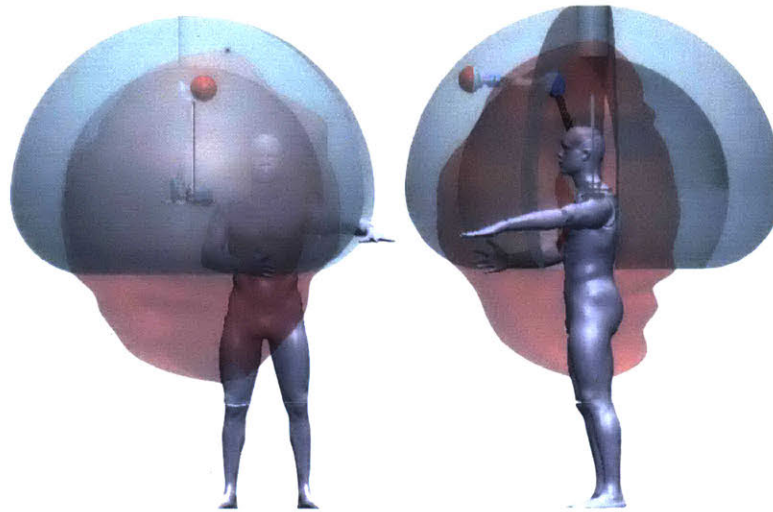


Figure 2-3: SRL Workspace with model of a person and the human arm workspace, repeated for reference

5.1.2 Initial and Previous Implementations

Figure 5-3 shows the first implementation of Aucto. This version is comprised of Dynamixel MX-106 motors which are controlled via RS-485 control signal. The sup-

porting structure is lightweight from the use of carbon fiber rods as links. The motors are attached to the links using 3D-printed brackets and couplings which join to the dynamixel aluminum mounting brackets sold with the MX-106's.

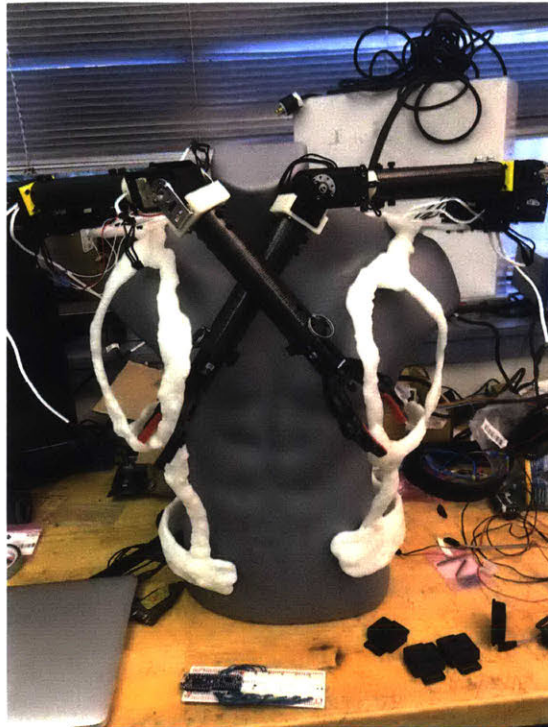


Figure 5-3: Aucto Mk.I with double arms of low strength that allowed for initial experimentation of trajectory control and the early tests of the ergonomic mounting and the direct control of movement.

This design was designed for minimum weight as possible to make Aucto safe via its low weight and low force. This version was built to begin implementation of trajectory control and for the initial analysis of controlling the system via direct control input.

Link lengths were chosen to leave the arms just short of human reach so that the robot would never extend beyond the human workspace. This way, the human wearer could always intervene in the process.

Figure 5-4 shows the next iteration. In this embodiment, the form factor for Aucto was implemented with a focus on safety. The arm joints were covered with custom stops that fully covered the actuators and mechanically limit the joint range.

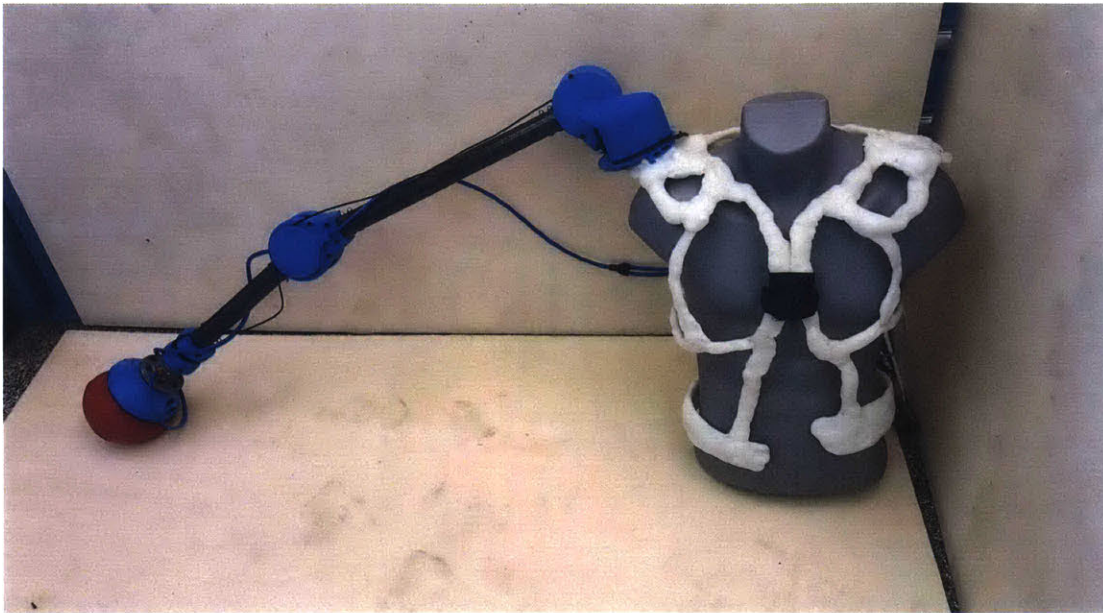


Figure 5-4: Earlier iteration of Aucto, showing the safety stops in assembly with the previous version of Joint actuators: double and single MX-106. The shoulder and arm joints are covered with the blue 3d-printed safety stops.

These stops are also present in the partial revision shown in Figure 5-5. A close up of these stops can be seen in Figure 5-6. The stops also act as guides for the pneumatic tubing that went to the gripper, and were designed as well to feed the power and communication cables of the motors through the hollow carbon fiber tubes.

In Figure 5-7 the next evolution of the shoulder joint was developed to increase strength. The metal brackets yield greater strength and durability over the prototypical, 3D-printed previous version. This version carried forward into the final implementation. The change was made after the functional requirements of the robot were updated to include handling larger workloads, and the opportunity to make a stronger SRL that could even support the wearer became evident.

To increase strength, the MX-106 motors were also swapped out with the much more effective Dynamixel Pro motors. The investigator found the MX-106s could not consistently support the torques for which they were rated. Therefore, the upgrade was immediately an evident necessity.

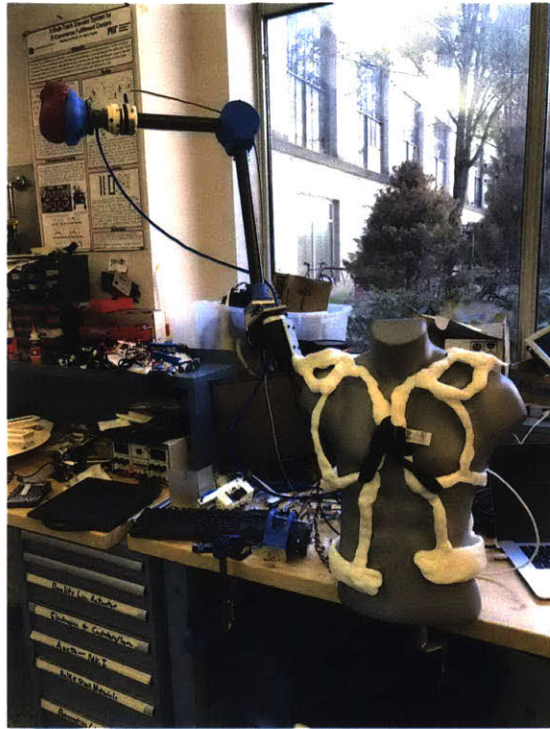


Figure 5-5: Later iteration of Aucto, showing the safety stops in assembly with the previous version of Joint 2 actuators: double MX-106

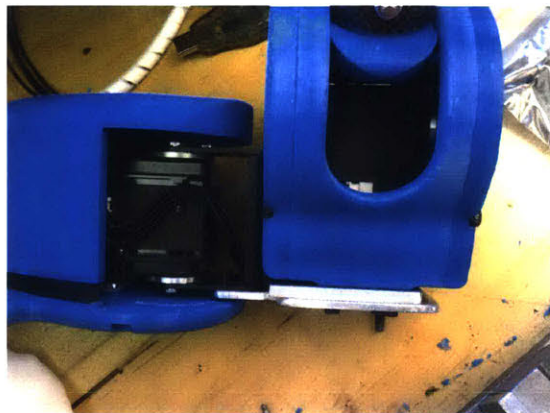


Figure 5-6: Close up of the safety stops of Aucto Mk.II. These safety stops constrain the movement of the joints to a limited range so that the workspace of the SRL never collides with the human wearer, especially the head of the worker.

5.1.3 Final Implementation of Mechanical Design

The current robot implementation is actuated by 3 Dynamixel Pro motors. The structure is comprised of carbon fiber tube links, with 3D-printed couplings that join

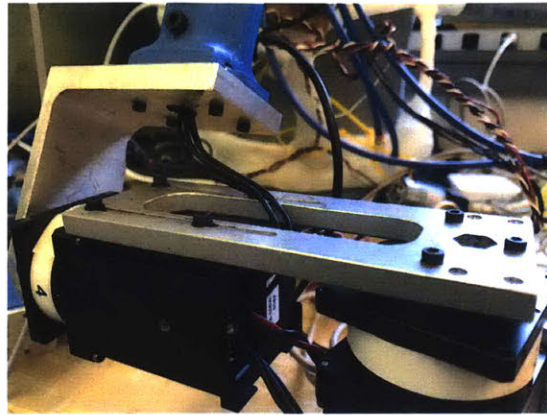


Figure 5-7: The shoulder joint of the Aucto SRL

to aluminum motor mounting brackets. This robot arm is mounted to the ergonomic body attachment via another aluminum mounting bracket which is embedded into the thermoplastic exoskeleton.

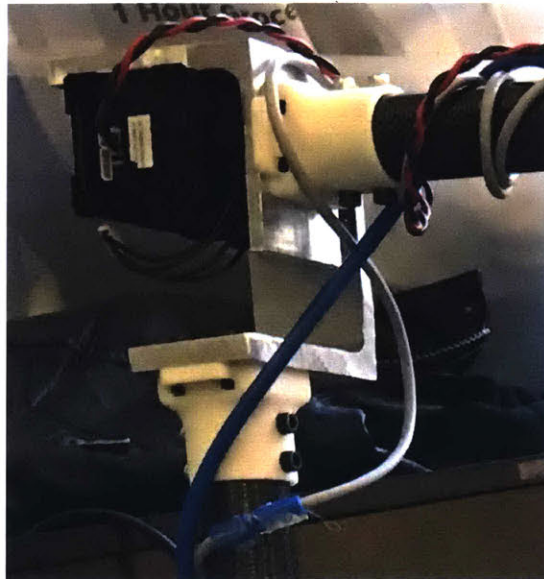


Figure 5-8: A close up view of a motor joint of Aucto with the carbon fiber tube couplings and the motor joint brackets

As the Dynamixels are capable of up to 70 NÅm of torque at peak (rated 25Nm cont.), the SRL can hold roughly 80N at full extension, but in the general workspace, if not constrained by software limits, it can apply 250-400N, this figure is of course dependent on configuration. The total mass of the arm prototype is 3.8 kg, with the

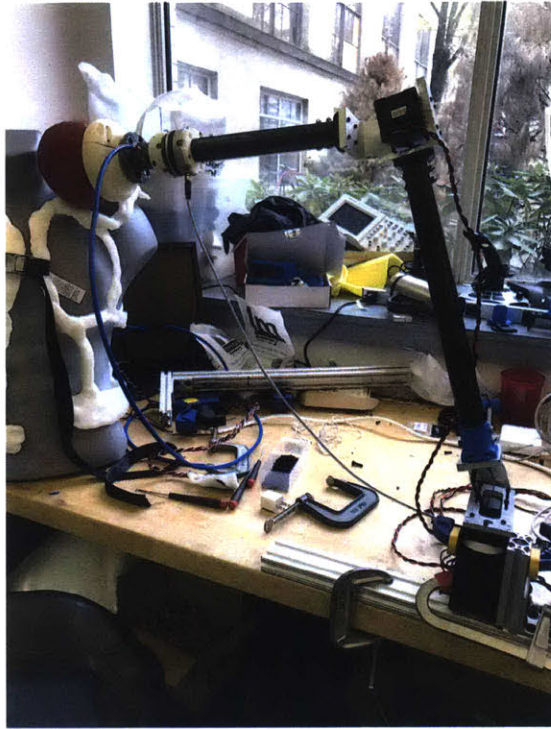


Figure 5-9: The final iteration of Aucto mounted in a testbed to test control systems without mounting to a human wearer

ergonomic attachment, battery, pump and other electronics on the full system is closer to 8 kg, however, that weight is mostly borne by the hip, and is fairly distributed across the body, such that, much like a hiking backpack, the added loads are more or less imperceptible.

Our control system allows us to conservatively send motor commands and read joint position at 250Hz, read from the force sensor at 1000Hz, and read from the IMU at 100Hz.

5.2 Electronics, Sensors, and Low Level Software

The control software is nearly entirely implemented in Python, with parallel processes managing sensor interface, joined into a main thread, interfacing together using the ZeroMQ library. We use the DynamixelSDK provided by Robotis to control the Dynamixels over serial with a Python wrapper for SDK which is implemented by Robotis

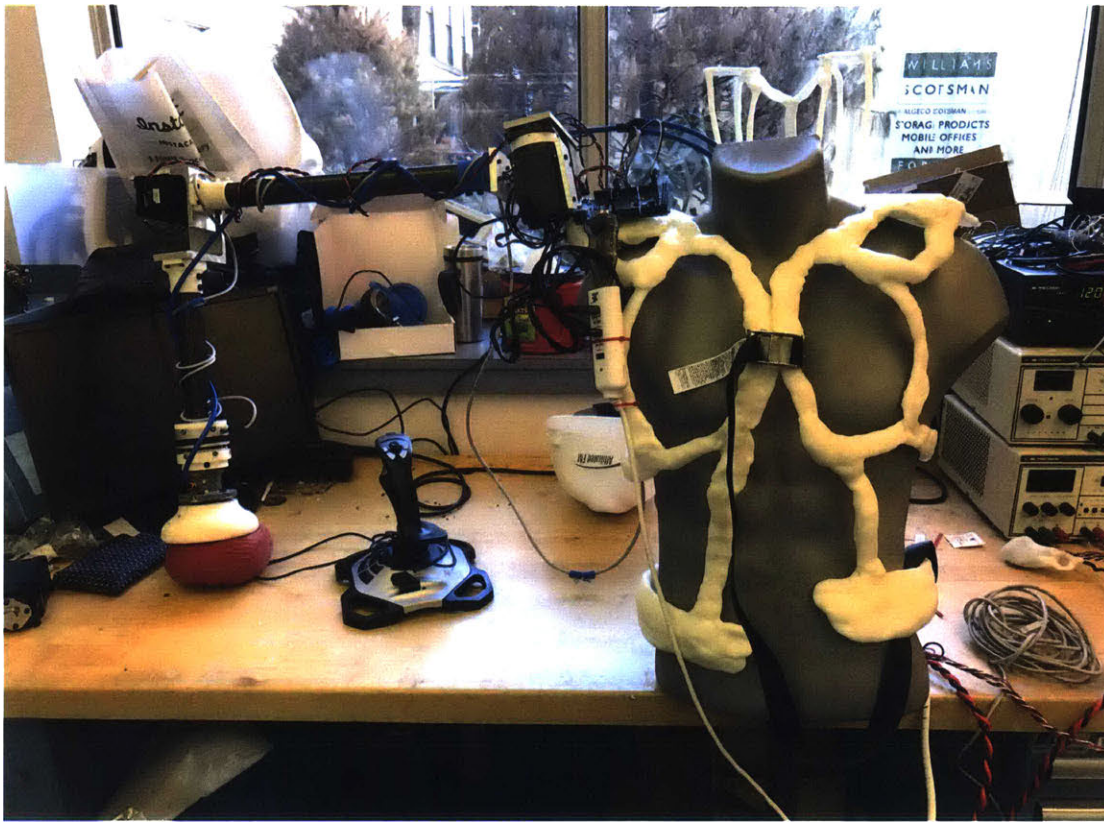


Figure 5-10: Final iteration of Aucto

in C. These motors are controlled via serial communication by a USB2Dynamixel Dongle and a series of 4-pin RS485 cables. Much of the speed of the overall control loop is accomplished by using C-libraries at the low level, and by developing the parallel process sensor interface, developed in part with Daniel Kurek[14], and affectionately dubbed miniROS. We found that we could consistently operate at 250Hz with no packet loss or loss of data. It is anticipated that further optimization could have pushed the system to much faster, and initial tests show that dynamixel's could be interfaced with combined read and write commands at 400-500Hz. This high-speed communication rate required low level resets of the USB drivers before running and could only be used on a Unix machine. The kernel of Windows likely does not allow for the USB interface to be prioritized. Eventually an embedded system or one with a Real-Time OS could be used to achieve the 500Hz interfacing. The difficulty of this speed is that we found packets would be dropped or the USB interface not

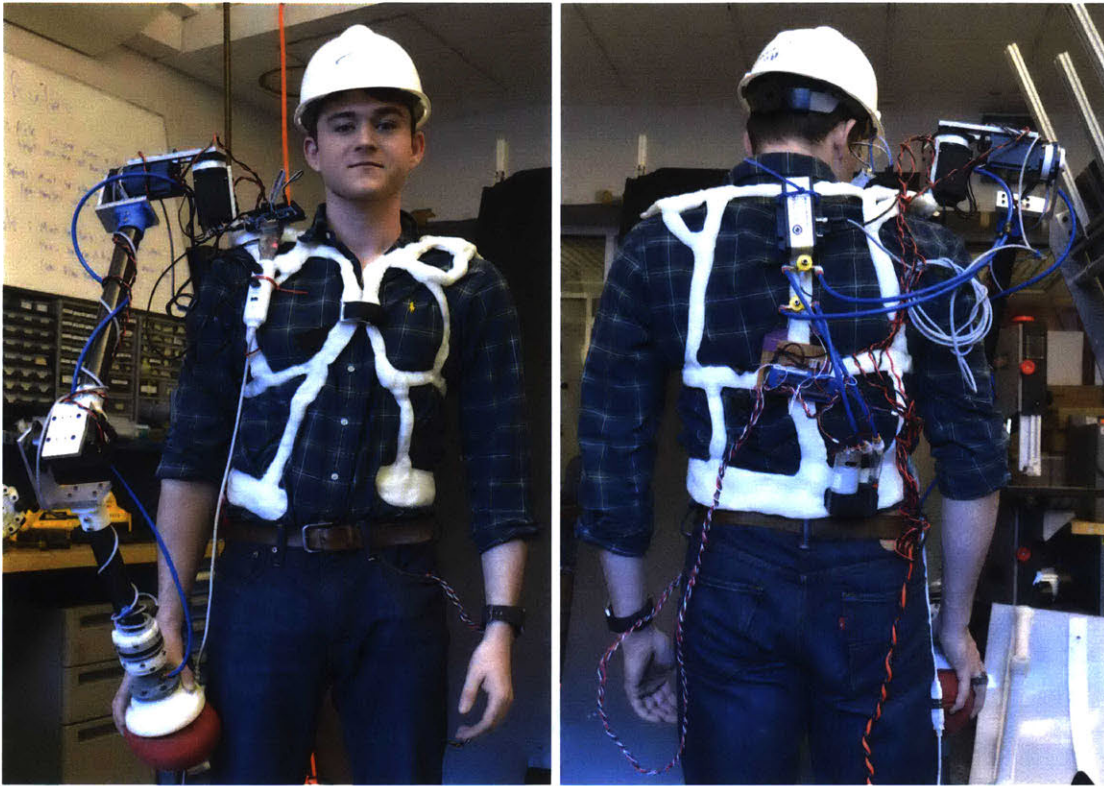


Figure 1-2: Repeated view of the Final Version of Aucto being worn, shown from front and back

immediately responsive. This issue is illustrated in Figure 5-12: the three datasets show a stark contrast of the before and after the correct manipulation of the serial ports is applied. High frequency of packet loss led to a mean time-to-read of 4.7ms, with delays as long as 17.7ms. By resetting the ports, we achieve a mean time-to-read of 2.3ms with two distinct bands of timing, one a 2ms and one at 3ms, this is due to the minimum driver latency of 1ms, and the fact that the base level OS is polling then at 1ms regularly, and so we have distinct 1ms intervals. This is itself an oversimplification of the mechanisms causing this at the low level, but such description is beyond the scope of this work.

The Optoforce sensor was interfaced with using a custom serial library; data was streamed at 1000Hz and filtered with a low pass with a cutoff frequency of 1.5Hz. The IMU is interfaced with using I2C with an Arduino acting as a serial-I2C adapter.

Data output is roughly 100Hz. A control joystick is interfaced with the pyGame library, which was effectively used as a SDL library wrapper, as this is the low level means of interface implemented in pyGame.

To expand on the parallel communication software we developed, “miniROS,” this is a use of the ZeroMQ networking library that re-implements a core functionality of ROS. The library allows for parallel asynchronous execution of multiple processes and a shared exchange of data from Publishers to Subscribers and all over local TCP/IP transactions. This allowed us to still work in python with the existing libraries on hand without the need to repackage into ROS, while allowing non-expert use of the program through simpler command line launches that could be readily executed in the prototyping phase as Python is an interpreted language. It is evident to the author that ROS has much of this functionality as well and uses Python as one of its main languages, but the speed of getting testable code was evident over the opportunity cost to get the same level of familiarity and flexibility in ROS.

In the implementation of the communication software developed, the sensors all publish their data streams asynchronously, and with a single item stack, i.e. any new data pushed will be the data read by the subscriber, and only one item is in the stack at a time. For the sake of safety control logic, the main loop contained all the motor

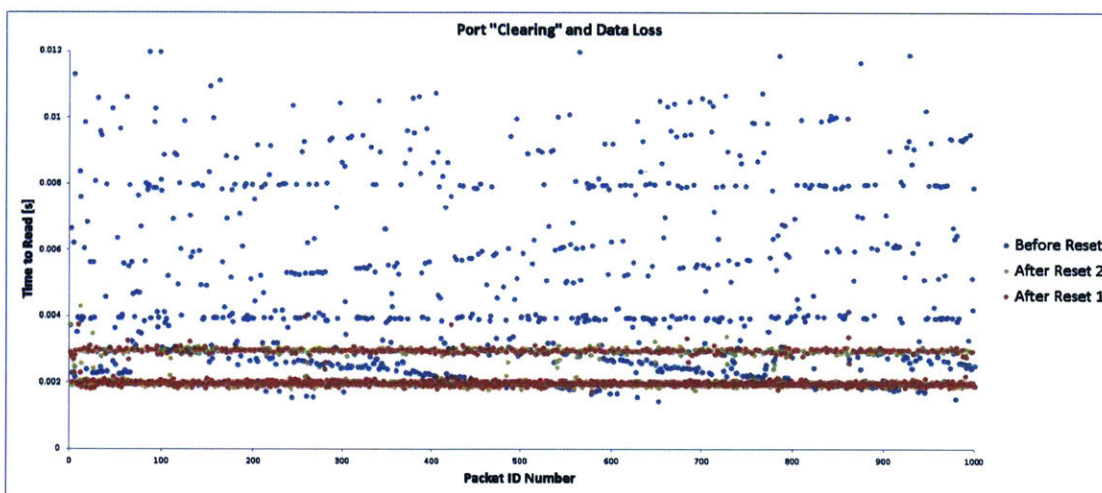


Figure 5-12: Serial Data transmission times, comparing the packet loss difference before and after “clearing” the port.

control logic, rather than having a separate process to govern the motors. However, there were separate processes and Publishers for the IMU, the Optoforce force sensor and the control Joystick used to override the control logic for the safety of the wearer or as general control input.

5.2.1 Force Sensor



Figure 5-13: The 6DOF Optoforce force sensor.

The sensor used in Mk. IIb/III of Aucto was the Optoforce 6D F/T sensor, the HEX-70-XE-1000N. The sensor has a max compression capacity of 1000N, tensile capacity of 450N, and shear force capacity of 200N in X-Y Plane; its capacity for torque is 6.5Nm in z and 10.5Nm about X and Y. Originally, we elected to use the lower cost 3-DOF sensor that was capable of measure linear force in X,Y and Z, however, initial tests showed that the sensor could not isolate the torque measurements and lead to inaccurate readings when the forces were applied off center or when torque, but no linear force, was applied. The upgrade allows for the sensor to specifically isolate the forces applied in X-Y-Z and prevents improper interpretation of torque as linear force.

The sensor is mounted inline with the links of Aucto. The sensor has an ISO standard flange which we mount to with custom 3D printed couplings shown in 5-14. The sensor is placed inline and as close to the gripper as possible to reduce the error introduced by the offset.



Figure 5-14: The couplings that mount the force sensor inline with the rest of the Aucto structure

5.3 Universal Gripper Design

Universal Granular jamming Grippers are a recently developed under-actuated gripper technology that leverages the phenomena of jamming media to grip objects. The principle of function is that you have an airtight container e.g. a balloon, full of grain or other media, and evacuate the air leaving a vacuum inside. The air pressure external to the container forces all of the grains together and they jam and lock in place. So, a bag full of loose granular media may be fluid at gauge pressure, but when at vacuum or at least partial vacuum, it becomes hard and stiff.

Figure 5-19 shows a prototype of Granular Jamming Gripper for the shoulder-mounted SRL. The gripper is made entirely of 3d printed components from a traditional Fused Deposition Modeling (FDM) printer. Only the “head” of the gripper needs to be airtight, this is typically made using stereolithography (SLA) but we achieve sufficiently airtight parts using post-processing of the FDM part. We em-

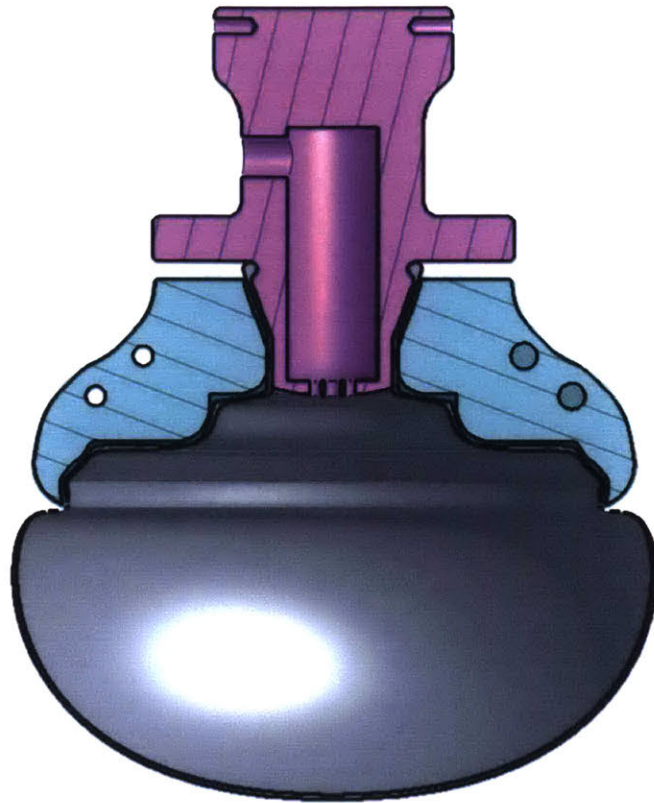


Figure 5-15: Cross section view of the Granular Jamming Gripper

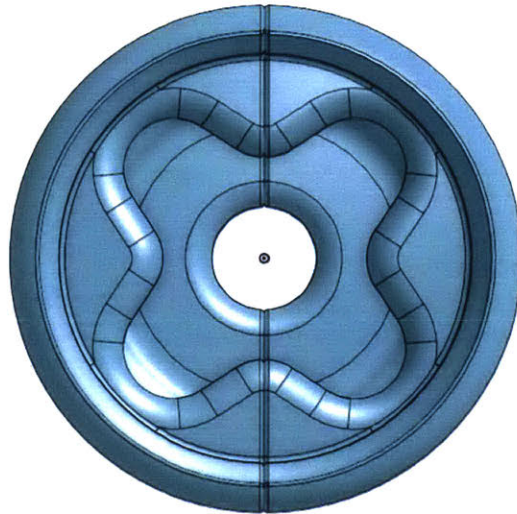


Figure 5-16: Bottom view of the Granular Jamming Gripper “cup” and the newly added torque holding feature.

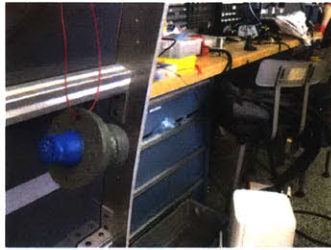


Figure 5-17: Sealing the Gripper “Head:” epoxy coat curing

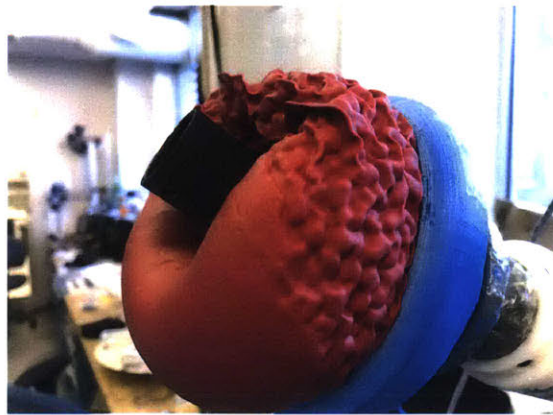


Figure 5-18: Close up view of the gripper with mixed media. The two different media textures, coffee vs. foam beads are visible, as is the separation between the two



Figure 5-19: The granular jamming gripper. The gripper is comprised of three parts: the head, the cup, and the balloon with media

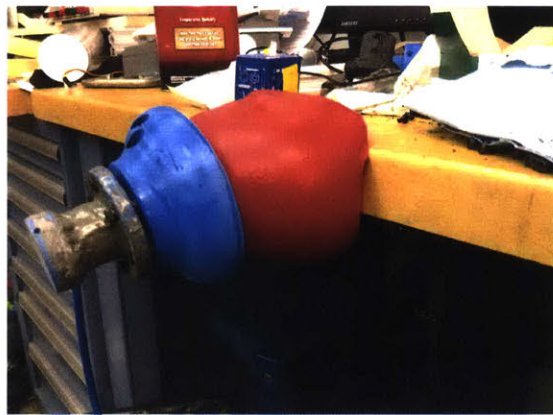


Figure 5-20: An example of the way the gripper takes the needed form to hold: a coffee only version of the gripper holds onto the work bench

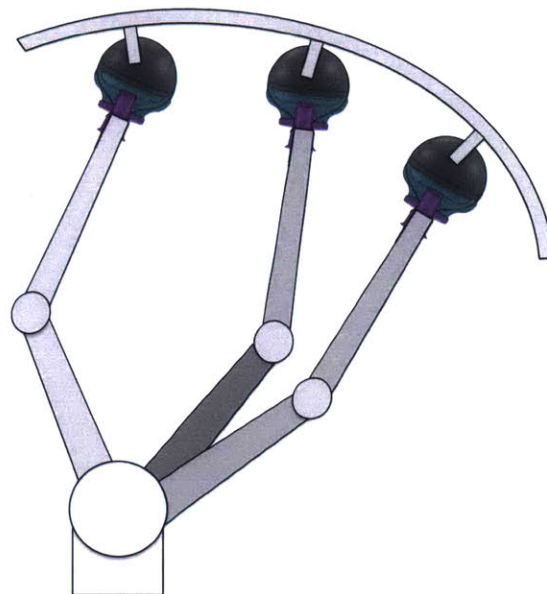


Figure 5-21: The granular jamming gripper allows for grasping or holding without the need to aim the gripper in 6DOF. The variety of orientations that can still allow for strong holding benefits Aucto to simplify the system to 3DOF

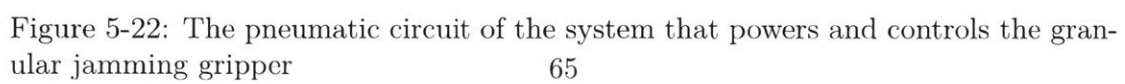
ployed acetone/solvent dipping as well as brush-on epoxy sealing to get an airtight seal in the head.

The “cup” is comprised of two mirrored parts that compress the latex balloon onto the head to seal the system more tightly and to allow for the load borne by the gripper to transmit into the links of the robotic arm. Note that the geometry of the cup has a lip to capture the balloon structure as well as a smooth, splined surface that dogs

with the jamming media when hardened. This shape is contrasted with the traditional form where the “cup” of the gripper is smooth and torque transmission relies on the material shear at the balloon-media interface as well as the adhesive seal between the 3d-printed “cup” and the outer surface of the latex balloon membrane. Figure 5-16 shows this new feature. The petal feature dogs with the granular media when it jams, therefore allowing for torque/shear to be supported by the gripper structure as opposed to the standard smooth features which rely on friction to prevent slip between the latex balloon and the gripper cup. Note as well that the cup is comprised of two symmetrical halves for ease of assembly. This additional feature allows for the cup to clamp over the balloon to form a better seal.

The granular jamming media used is a mix of hard Styrofoam pellets and ground coffee. This gives the high performance of coffee as a granular media, but is 10-20% the weight of the same volume of only coffee. Using a small 12V DC diaphragm pump, we pull the needed 15” Hg of vacuum for jamming, up to 20” Hg. The pump also allows for positive pressure or inflation.

To control the pump to either increase or decrease the media balloon pressure, the pneumatic circuit shown in Figure 5-22 was designed. This was then realized as shown in 5-23, using a set of pneumatic control valves, and a pair of toggle switches which were molded into the remote control shown in Figure 5-24. One switch activates the pump, and the other switch controls the airflow direction by switching each valve on or off.



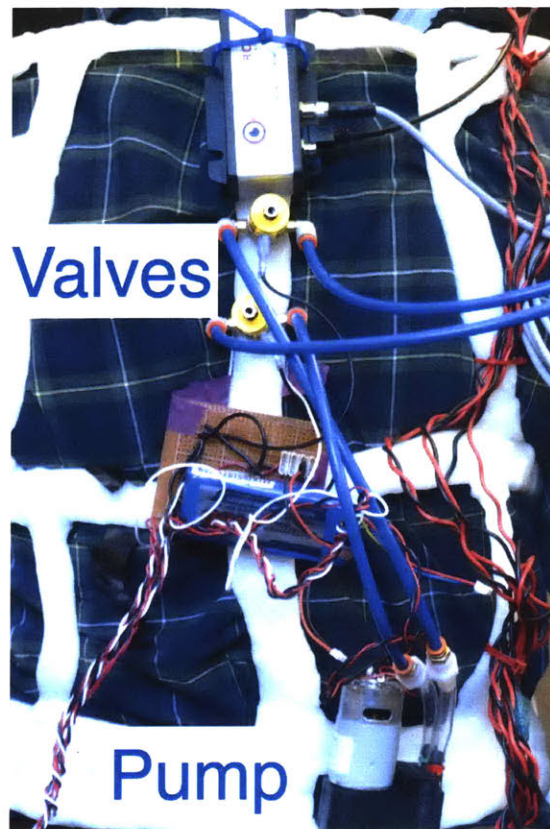


Figure 5-23: A close-up view of the pneumatic valves and circuit as implemented in the Aucto prototype



Figure 5-24: The handheld control switches that govern the operation of the granular jamming gripper by running the pump and selecting the direction of flow.

Chapter 6

Controls System

6.1 Control Laws and Algorithms

6.1.1 Coordinate Systems and Motion Compensation

Despite the salient feature of the shoulder-mounted SRL, the control of the robot is inevitably more challenging. Since the SRL is mounted on the shoulder of a human, movements of the human continually disturb the robot. Unlike a robot sitting on a floor, or an assisting worker standing next to the main worker, the SRL is on a moving base. As shown in Figure 6-1 the base coordinate frame is attached to the shoulder of the human where the SRL is secured. Viewed from the world coordinate frame, the base frame moves as the human moves. The base movement acts as an exogenous disturbance to the control system of the SRL. The SRL control system must be able to compensate for the human movement disturbance.

Furthermore, in the context of the aircraft fuselage assembly, the worker will change the posture for picking up their tools, e.g. a screwdriver, and affix the plate being held by the SRL with fasteners. The SRL should not impede the human motion, but allow the human to move freely, while the plate must be held stably despite the human movements.

A naïve method for compensating for human movements is to measure the human position and orientation, and move the SRL in the opposite direction to the movement

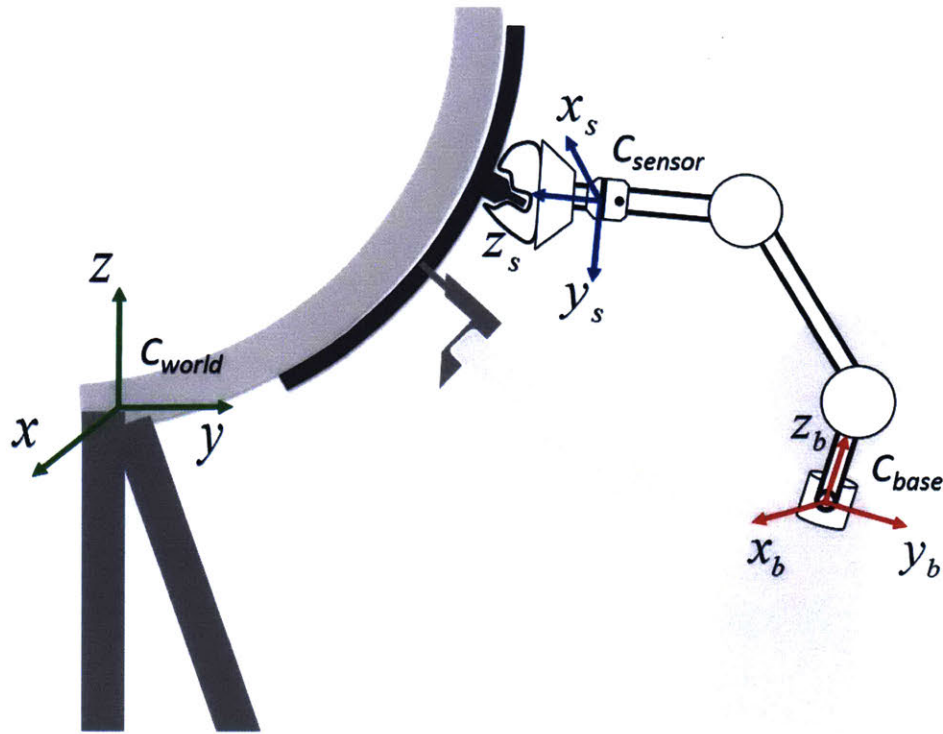


Figure 6-1: SRL Workspace with model of a person and the human arm workspace

of the human. This method did not work for two reasons. One is that the human body motion is highly complex, and difficult to measure with a high spatio-temporal resolution. Second, since the object must be securely held with SRL, it must be pressed against a fixture or the ceiling. This requires controlling the force with which the SRL is holding and supporting the object at the tip. In general, force feedback loop needs a higher bandwidth, which is difficult to achieve with positional feedback signals. Therefore, we implement admittance control as the main compensation of motion, further explored in Section 6.1.3.

However, the postural changes of the wearer are not compensated for in a simple admittance controller: as the robot base moves with the wearer, the direction of force changes with respect to the robot coordinate system. As shown in Figure 6-1, the coordinate systems are all moving except the world coordinate system. It is in the world coordinate system that we want to maintain the constant force of the admittance control. Therefore, in the calculation of the admittance control, we must

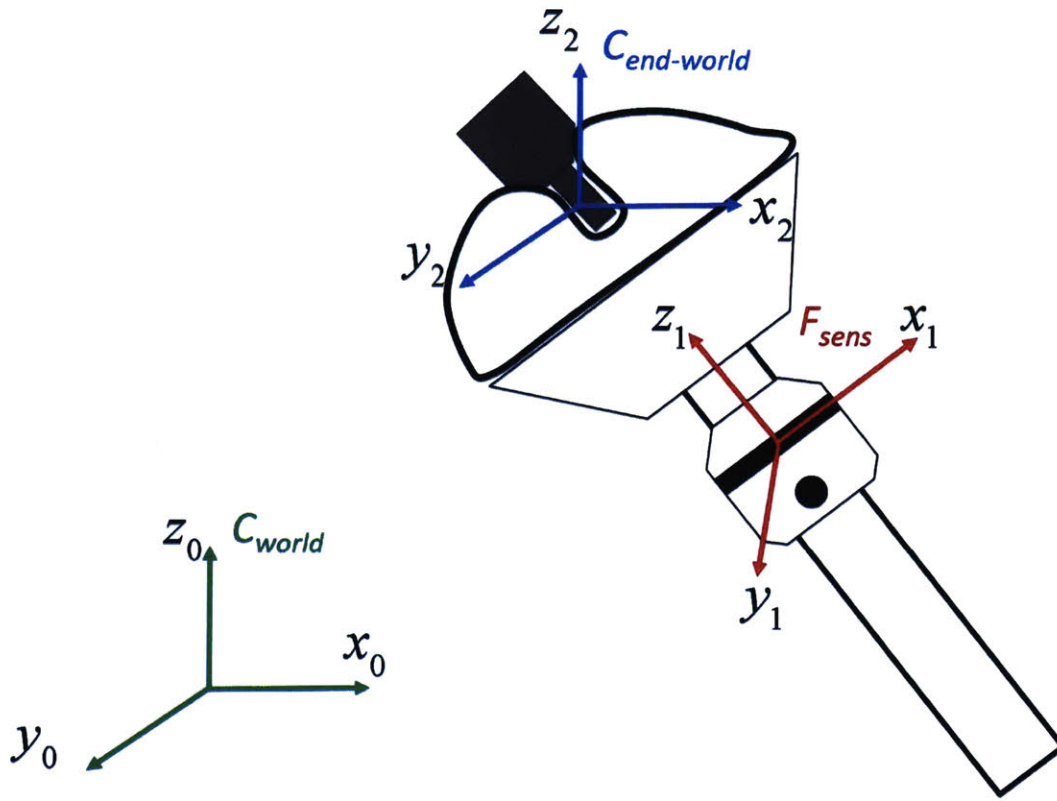


Figure 6-2: The coordinate systems of the gripper

compute the forces in the world coordinate system to compare against the original setpoint force, then map this back into the robot coordinate system to command the velocities of the joints to compensate the force changes.

We use the sensor package described in Section 3.1.2 to measure the orientation of the robot base.

We compute the orientation of the force sensor from the kinematics of the robot directly.

$$x_{sens} = \begin{bmatrix} s_1 \\ c_1 \\ 0 \end{bmatrix}, y_{sens} = \begin{bmatrix} -s_1 s_{23} \\ c_1 s_{23} \\ s_{23} \end{bmatrix}, z_{sens} = \begin{bmatrix} -s_1 s_{23} \\ c_1 s_{23} \\ c_{23} \end{bmatrix}$$

From the vectors of the Force Sensor coordinate system, and an understanding of the offset of the gripper and changing coordinates as shown in Figure 6-2, we can

map the force sensed to the world coordinates as follows':

$$\begin{aligned}\vec{F}_{world} &= \mathbf{R}\vec{F}_{sensor} \\ \vec{M}_{world} &= \mathbf{R}\vec{M}_{sensor} + \vec{r} \times \vec{F}_{sensor}\end{aligned}$$

Where $\vec{r} = l_{sens2Grip}\vec{z}_{sens}$, and

$$\mathbf{R} = \begin{bmatrix} c_{11} & c_{12} & c_{13} \\ c_{21} & c_{22} & c_{23} \\ c_{31} & c_{32} & c_{33} \end{bmatrix}$$

And where $c_{ij} = \cos(\angle \mathbf{X}_{sens_i} \mathbf{X}_{world_j})$, with $\mathbf{X}_{sens_2} \equiv \vec{y}_{sens}$

$$\begin{aligned}c_{11} &= \frac{\vec{x}_{sens} \cdot \vec{x}_{world}}{||\vec{x}_{sens}|| ||\vec{x}_{world}||}, c_{12} = \frac{\vec{x}_{sens} \cdot \vec{y}_{world}}{||\vec{x}_{sens}|| ||\vec{y}_{world}||}, c_{13} = \frac{\vec{x}_{sens} \cdot \vec{z}_{world}}{||\vec{x}_{sens}|| ||\vec{z}_{world}||}, \\ c_{21} &= \frac{\vec{y}_{sens} \cdot \vec{x}_{world}}{||\vec{y}_{sens}|| ||\vec{x}_{world}||}, c_{22} = \frac{\vec{y}_{sens} \cdot \vec{y}_{world}}{||\vec{y}_{sens}|| ||\vec{y}_{world}||}, c_{23} = \frac{\vec{y}_{sens} \cdot \vec{z}_{world}}{||\vec{y}_{sens}|| ||\vec{z}_{world}||}, \\ c_{31} &= \frac{\vec{z}_{sens} \cdot \vec{x}_{world}}{||\vec{z}_{sens}|| ||\vec{x}_{world}||}, c_{32} = \frac{\vec{z}_{sens} \cdot \vec{y}_{world}}{||\vec{z}_{sens}|| ||\vec{y}_{world}||}, c_{33} = \frac{\vec{z}_{sens} \cdot \vec{z}_{world}}{||\vec{z}_{sens}|| ||\vec{z}_{world}||}\end{aligned}$$

Further, the final algorithm shown in Section 6.1.4 reflects the overall use of these formulae and coordinate mappings.

6.1.2 Torque Control of SRL

In the process of designing the control algorithms for Aucto, we construct a torque control based approach. This was a logical solution to the problem as it would allow for the control of force at the end effector more directly without much worry for dynamics, while simultaneously allowing for simple compensation for system dynamics that is computationally cheap and numerically stable.

Here, we still calculate the difference between the measured and setpoint force:

$$\Delta \vec{F} = \vec{F}_{setpoint} - \vec{F}_{meas}$$

However, we additionally use a PI controller to send an effective “effort” of force command signal to the torque control algorithm, this includes windup compensation in the integrator for the force signal:

$$\Delta \vec{F}_I = \begin{cases} \Delta \vec{F}_I + \Delta \vec{F} \delta t & -10 < \Delta \vec{F}_I + \Delta \vec{F} \delta t < 10 \\ -10 & \Delta \vec{F}_I + \Delta \vec{F} \delta t \leq -10 \\ 10 & \Delta \vec{F}_I + \Delta \vec{F} \delta t \geq 10 \end{cases}$$

$$\vec{F}_{PI} = K_p \Delta \vec{F} + K_i \Delta \vec{F}_I$$

$$\vec{F}_{effort} = \vec{F}_{setpoint} + \vec{F}_{PI}$$

Then, we compute \vec{F} , which is the end effector force component of the torque commanded, i.e. this is the torque in each of the joints which would result in a force $vecF_{effort}$:

$$\vec{F} = \mathbf{J}^T \vec{F}_{effort}$$

Finally, we compute the torque signal to command to the motors, this includes compensation for the Inertia, \mathbf{H} , Coriolis torques, \mathbf{C} , damping, \mathbf{D} , and the weight or effect of gravity to torques at each joint, \vec{G} :

$$\vec{T} = \vec{F} + \mathbf{H} \frac{d^2 \vec{Q}}{dt^2} + \mathbf{C} \frac{d \vec{Q}}{dt} + \mathbf{D} \frac{d \vec{Q}}{dt} + \vec{G}$$

See Appendix A for any non-trivial formulae not included elsewhere in this text.

This torque command is then sent to the motors at the fastest frequency manageable to allow for real-time torque compensation.

The difficulty in the implementation of this algorithm was inevitably the stability of the models generated for sending torque commands to the motors elected for use: the Dynamixel Pro series, and originally the Dynamixel MX-106s as well. Without the implementation of custom electronics, we found it exceedingly and prohibitively difficult to implement a torque control loop to these motors. The difficulty of this is that the serial command signals allow for a current signal command that sadly

is not implemented for use at high frequencies. We found that in both series of motor the Back EMF and the back EMF compensation of the motors made too great of an impact for the motors to effectively be commanded via torque control. In fact, we ran extensive tests attempting to characterize these motors. Theoretically, our model came very close to modeling the friction inside the motors, however, the raw data output was highly oscillatory and difficult to work with in high frequency control. This came about as a result of the current sensing module measuring the current supplied to the Pulse Width Modulated DC signal that was fed to the motors from the transistors. We found that the current measured could be filtered, but the problem was in being able to consistently command torque commands to the motors, a proper characterization of the friction of the system became very difficult, and we elected to focus solely on the admittance controller that was being developed.

However, in future work, these same control laws would be quite useful in a similar system and if the torque controller of the motor is sufficiently stable, the dynamics of the SRL-Human system could be much more effectively compensated.

6.1.3 Admittance Control for SRL

Here we propose a force control method integrated with admittance control. Instead of measuring the human motion, we measure the force acting between the object being held and the wrist of the gripper, that is, the force that the SRL is applying to the object. To support the plate against gravity and assure that the plate is securely pressed against the ceiling or a fixture, the SRL must maintain a certain level of force or a reference force, continuously. As shown in Figure 6-3, a force feedback loop is formed around the endpoint force sensor. This force control system must not be disturbed by human movements, yet the SRL must accommodate the human desire to change the posture. To meet these requirements, we consider the following admittance control represented in the world coordinate system: $\vec{v} = \mathbf{A}\Delta\vec{F}$

where \mathbf{A} is an admittance matrix to be specified, \vec{v} is a commanded velocity of the end-effector, and $\Delta\vec{F}_{SRL}$ is the difference between the reference and measured endpoint force: $\Delta\vec{F} = \vec{F}_{meas} - \vec{F}_{setpoint}$

Suppose that the human attempts to move away from the gripping point of the object P_G . See Figure 6-1 Then the endpoint force of SRL tends to reduce, which is detected by the force sensor. This induces the velocity command proportional to the reduction of the endpoint force, according to the admittance control law. The higher the admittance matrix value, the faster the SRL movement in pushing back the endpoint, so the endpoint force recovers. This is the simplest control algorithm that worked well, as demonstrated later in the experiment section. There are a few important points to remark, however.

Under-actuation: Recall that the shoulder-mounted SRL does not have a three-axis powered wrist. Thanks to the Granular Jamming Gripper, the SRL can grasp an object from an arbitrary direction, eliminating the need for a heavy powered wrist. This makes the SRL lighter and simpler, but it makes the system “under-actuated”. Fortunately, however, the Granular Jamming Gripper exhibits a significant rotational compliance with which it grasps an object. As the human attempts to move sideways, for example, the SRL responds to the change of the endpoint force and compensates for it by changing its configuration. This tends to change the orientation of the upper arm, resulting in a moment at the gripper. This resistive moment is small within $\pm 20^\circ$ or so, although it varies depending on the shape of the object and the suction pressure of the Granular Jamming Gripper.

Natural Haptic Feedback: It is interesting to note that the force applied by the SRL to the object is sensed by the human through the arm links and base of the SRL. Since the SRL is mounted on the shoulder of the human, all the reaction forces act on the human. This forms a “natural” haptic feedback from the contact point of the SRL to the human shoulder. Without using any active means, the human can sense and monitor the reaction force at the endpoint. In case the reaction force drops due to the human movement, it gives a warning to the human that the object being pressed against the ceiling is about being detached. Although difficult to quantify the human sensation, it has been observed through experiment, that the human can check whether the object is properly held and accommodate his/her motion to maintain the

contact. Refer back to Section 4.3 for more.

Low-Level Control: Based on the admittance control law and the measurement of contact force, the desired endpoint velocity is determined in the world coordinate system. The SRL control system must be able to execute this velocity command faithfully. This is a standard low-level robot control problem, which has been addressed in the literature [24]. However, a few critical implementation issues are worth mentioning. First, the velocity command needs to be resolved to joint velocities with the Jacobian inverse. Near singularity, however, this causes an unwanted behavior. To alleviate this, the singularity-robust, inverse kinematics formulation is effective [32]. Second, a force feedback loop, in general, requires a higher sampling rate. In our case, the system tends to be unstable for an aggressively large admittance, which requires a large velocity for a small force discrepancy. Given a limited sampling rate of the force sensor, this may cause instability, as discussed further in the implementation and experiment sections.

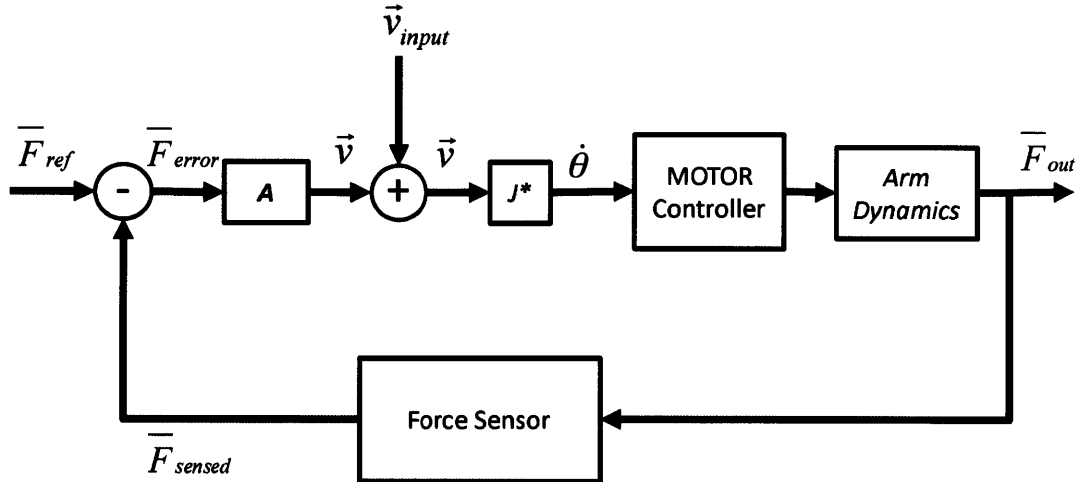


Figure 6-3: Block Diagram of the control loop

Lastly, we identify that there is a setpoint force needed for our control algorithm. This setpoint force was established in practice by setting the force manually at the start of the trials. The wearer applies the desired setpoint force for 2-4 seconds in the correct direction while Aucto takes 1000 samples of data, and averages the

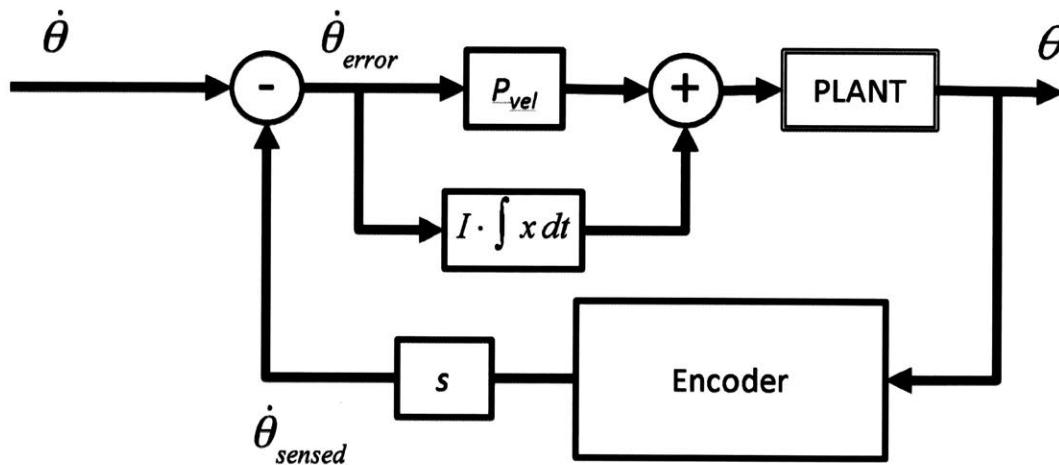


Figure 6-4: The low level control loop operating inside the Dynamixel Pro motors. This was reverse engineered experimentally to decipher the control loop, so there may be slight differences in the true implementation by Robotis

final results to yield a setpoint force in a certain direction. This procedure was implemented as it gives a great flexibility to the tasks that Aucto can complete; however, in the future, pre-programmed forces may be used, the system could use a control input that commands a certain amount of force via user input or some other control scheme. There are many future options, but we elect the simplest and most intuitive interaction: the wearer pushes the arm against and object or surface with the desired force, and Aucto maintains that force once calibration is complete.

6.1.4 Final Algorithm Implementation

While the final control software was implemented in python, we enumerate below the pseudo-code for the main control loop which additionally includes the set-up procedure.

Algorithm for final version

```
# Start initial Calibration


$\mathbf{p}_{start}$  = getIMUData()


for 1000 samples:
    # Collect data from sensor publishers
```

```

pcurrent = getIMUData()
 $\vec{Q}$  = getMotorPosData()
pBase = pstart-1 * pcurrent
Fsens = getForceSensorData()

# Calculate Orientation of sensor WRT base
 $\vec{x}_{sens} = \begin{bmatrix} s_1 \\ c_1 \\ 0 \end{bmatrix}$ 

 $\vec{y}_{sens} = \begin{bmatrix} -s_1 s_{23} \\ c_1 s_{23} \\ s_{23} \end{bmatrix}$ 

 $\vec{z}_{sens} = \begin{bmatrix} -s_1 s_{23} \\ c_1 s_{23} \\ c_{23} \end{bmatrix}$ 

# Calculate Orientation of sensor WRT world coordinates by rotating by base orientation
quaternion

 $\vec{x}_{sensrot} = \mathbf{p}_{Base} * \vec{x}_{sens} * \mathbf{p}_{Base}^{-1}$ 
 $\vec{y}_{sensrot} = \mathbf{p}_{Base} * \vec{y}_{sens} * \mathbf{p}_{Base}^{-1}$ 
 $\vec{z}_{sensrot} = \mathbf{p}_{Base} * \vec{z}_{sens} * \mathbf{p}_{Base}^{-1}$ 

# Get rotation matrix representation of sensor orientation
 $\mathbf{R} = \begin{bmatrix} c_{11} & c_{12} & c_{13} \\ c_{21} & c_{22} & c_{23} \\ c_{31} & c_{32} & c_{33} \end{bmatrix}$ 

# Calculate Force in World Coordinates by rotating sensor data
 $\vec{F}_{meas}[i] = \mathbf{R} \vec{F}_{sens}$ 
 $\vec{F}_{setpoint} = \text{average}(\vec{F}_{meas}[:])$ 

# Begin Main Loop
while True:

    # Collect data from sensor publishers

```

```
pcurrent = getIMUData()
```

```
 $\vec{Q}$  = getMotorPosData()
```

```
pBase = pstart-1 * pcurrent
```

```
Fsens = getForceSensorData()
```

```
# Calculate the DLS Inverse Jacobian, using manipulability, w, and damping factor,  $\lambda$ 
```

```
J = jacobianOfEndeffector( $\vec{Q}$ )
```

```
w =  $\sqrt{\det(\mathbf{J}\mathbf{J}^T)}$ 
```

```
wthresh = 0.05
```

```
 $\lambda_{max}$  = .1
```

```
 $\lambda = [[w < w_{thresh}]]\lambda_{max} \left(1 - \frac{w}{w_{thresh}}\right)^2$ 
```

```
JDLS-1 = JT((JJT) +  $\lambda\mathbf{I}$ )-1
```

```
J* = JT((JJT) +  $\lambda\mathbf{I}$ )-1
```

```
# Check that EStop from Joystick not engage and proceed
```

```
if checkJoystickInputOK():
```

```
    # Get offset manual control input
```

```
    xyzJoystickCommand = getJoystickInputData()
```

```
# Calculate Orientation of sensor WRT base
```

$$\vec{z}_{sens} = \begin{bmatrix} -s_1 s_{23} \\ c_1 s_{23} \\ c_{23} \end{bmatrix}$$

$$\vec{x}_{sens} = \begin{bmatrix} s_1 \\ c_1 \\ 0 \end{bmatrix}$$

$$\vec{y}_{sens} = \begin{bmatrix} -s_1 s_{23} \\ c_1 s_{23} \\ s_{23} \end{bmatrix}$$

```
# Calculate Orientation of sensor w.r.t. world coordinates by rotating by base
```

orientation quaternion

$$\vec{x}_{sensrot} = \mathbf{p}_{Base} * \vec{x}_{sens} * \mathbf{p}_{Base}^{-1}$$

$$\vec{y}_{sensrot} = \mathbf{p}_{Base} * \vec{y}_{sens} * \mathbf{p}_{Base}^{-1}$$

$$\vec{z}_{sensrot} = \mathbf{p}_{Base} * \vec{z}_{sens} * \mathbf{p}_{Base}^{-1}$$

Get rotation matrix representation of sensor orientation

$$\mathbf{R} = \begin{bmatrix} c_{11} & c_{12} & c_{13} \\ c_{21} & c_{22} & c_{23} \\ c_{31} & c_{32} & c_{33} \end{bmatrix}$$

Calculate Force in World Coordinates by rotating sensor data

$$\vec{F}_{meas} = \mathbf{R} \vec{F}_{sens}$$

Calculate difference from setpoint

$$\Delta \vec{F} = \vec{F}_{meas} - \vec{F}_{setpoint}$$

Calculate Force in Robot Coordinates by rotating command by inverse of the Base

Orientation

$$\Delta \vec{F}_{SRL} = \mathbf{p}_{Base}^{-1} * \vec{F}_{command} * \mathbf{p}_{Base}$$

Calculate the command velocity by multiplying by admittance, α

$$\vec{v} = \mathbf{A} \Delta \vec{F}_{SRL}$$

Calculate the command angular velocity by multiplying by DLS inverse Jacobian

$$\dot{q} = J_{DLS}^{-1} \vec{v}$$

$$\dot{q} = J^* \vec{v}$$

if the motor exceeds the correct range of motion, change velocity to send it back

into the correct workspace

if motorOutOfRangeLow for all Motors:

$$dq[motor] = 0.1$$

if motorOutOfRangeHigh for all Motors:

$$dq[motor] = -0.1$$

Send Command signal to motors

writeMotorVelocityCommand(dq)

Chapter 7

Testing, Results and Performance

Here, we summarize the final performance of the completed prototype. A video demo of the device can be found here: <https://youtu.be/WWJXtVTjvcA>

7.1 Testing–Experimental Procedure

As outlined prior, there are many tasks for which the SRL is useful. Figure 2-1. shows the Overhead Assembly task, and Figure 7-1. shows the other tasks used to evaluate the SRL, the Crouching Support task, the Simple Force Holding task, and the Mock Tool Support task.

To clarify the specifics of each task and others done:

Overhead Assembly – The wearer sets up the manufacturing task with the SRL and uses the force control of the robot arm to support the overhead compartment while they affix the compartment with fasteners. During this task, the person must move around and back and forth, as well as change orientation, pick up or move tools, etc. The SRL must be able to maintain contact with and hold up the Overhead Compartment as the wearer bolts it in place. We simplify this task by starting from a configuration where the compartment has already been lifted by the worker, and can use some locating features to partially support the workpiece, as shown in Figure 2-1.

Crouching Support task – The worker is kneeling on the ground for some manu-



Figure 7-1: The Various Tasks: A) Crouching, Supported by SRL instead of own hands, B) Simple Force Holding, Pushing with Force Against Structure only, C) Supporting a Mass at the Gripper for Assisted Tool Holding or Manipulation

facturing task, e.g. cable routing, floor panel assembly, inspection, picking parts etc. The concept is that rather than the human supporting themselves with their hands, which would limit their dexterity and productivity, the SRL can hold the person up and allow both hands free to work. The wearer will shift their weight around and move up and down, side to side, and introduce oscillations to see if the SRL can stably support them. Simple Force Holding task – The SRL gripper directly interfaces with a freestanding, sturdy structure. The force of the robot is directly loaded to the stiff structure. The wearer then moves around, back and forth and does so with varied movements, introducing oscillations to prompt frequency response, or rapidly moving away from the structure to see if the SRL will continue to correctly apply force.

Mock Tool Support task – This task as mentioned before is meant to mimic the use of isoelastic arms in manufacturing tasks, such as the Fortis, or Robo-Mate. For our example, the robot supports a free mass of 2.27 kg. The wearer will make the gripper hold the mass, then the wearer allows only the weight of the mass to apply force to the robot arm; the set point force is the weight of the mass, directed in the axis of gravity in the world coordinates, allowing for the weight to be supported and compensated for by the SRL. If the wearer inputs any additional force, the admittance controller acts to move the object in the direction of the disturbance force applied, making the tool weightless from the perspective of the wearer in the same vein as an isoelastic arm with the weight borne in the legs of the wearer.

An additional experiment was conducted to test the accuracy of the SRL’s sensors and control to compensate and track the posture of the wearer. In this task, properties of the Singularity Robust Inverse Jacobian[32] were used to make the robot arm always point along the X-axis. As the human wearer turns in Yaw as part of the trial, the robot must turn the base shoulder joint, θ_1 , to compensate. This gives us a direct measure of accuracy of the tracking in the control loop and the response time.

7.1.1 Human Haptic Feedback and Proprioception

Very simple blind tests were performed to qualitatively explore the efficacy of the haptic feedback performance of the SRL. After some short time of practice and learning is undergone, the wearer can successfully identify the direction of force and torque on the end effector and can blindly touch to the end effector while blindfolded.

7.2 Force Control Tracking and Holding

During the various experiments and trials, the force applied to the structure, tool, workpiece etc. was maintained consistently, and the gripper remained in contact, applying force and never dropping or releasing the engagement as long as the admittance was tuned to the optimal value for the task. In Figure 7-2. note the highlighted regions which show that the deviation during most of the operation is roughly $\pm 2\text{N}$. The large increases and decreases in force are from large changes in movement of the system, as the admittance controller commands velocity based off the force deviations.

The force data in the Overhead Compartment task shown in Figure 7-3 contains a similar trend of small deviations except in the case of large velocity disturbances. During the completion of the task, the robot arm stays engaged with the overhead compartment the entirety of the task. As well, no failures or releases were caused by large or fast movements by the wearer. The Worker wearing the robot arm is not impeded by the position or motion of the robot arm either, and free motion is possible, as the worker could complete the entire manufacturing task easily.

Figure 7-6. shows the forces measured in the world coordinate frame during parts of each task as well; the dynamics of the control loop remain consistent throughout these trials, as the robot maintains good holding and applies consistent force without impeding human motion in all the tasks. This figure specifically references data from the mock tool holding trials; however, this is demonstrable of the patterns seen in much of the data collected.

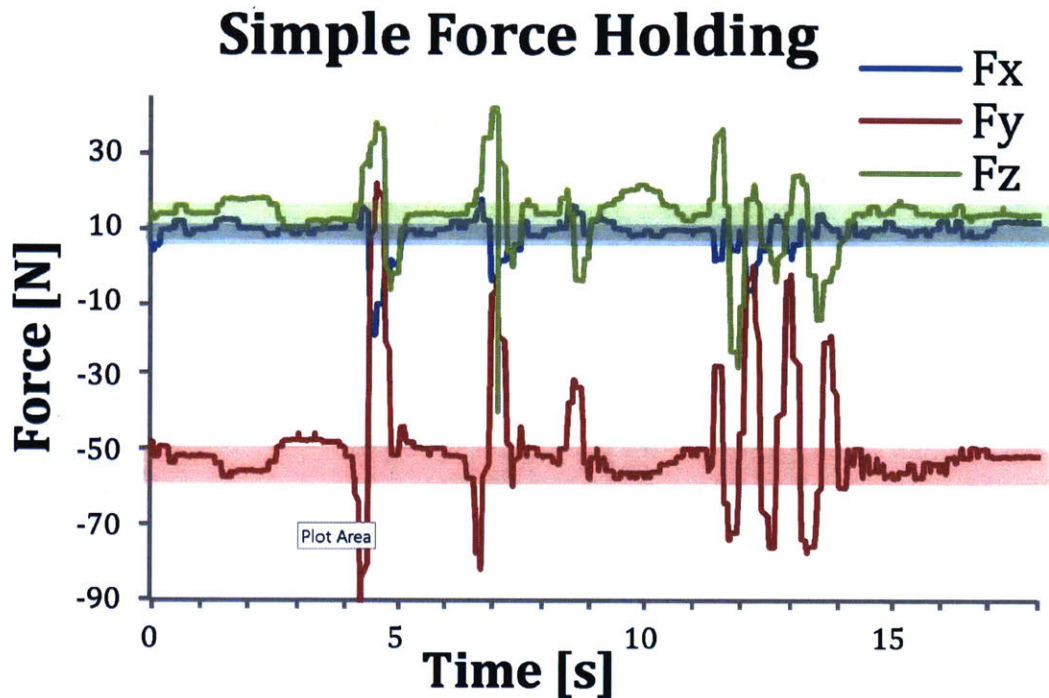


Figure 7-2: Force Measured During a Simple Force Holding Task (Admittance = 0.04m/s/N) Highlighted: small deviations of only a few newtons unless the system is doing fast velocity compensation

7.3 Admittance Tuning

By tuning the admittance of the control loop, one can tune the system for specific tasks that have different requirements. In systems where we would want the robot to be very damped and stiff, the system prevents the wearer from deviating from the correct position quickly. This is effective in some situations, but in general cases like ours, we prefer to allow free movement for the wearer. As well, we must be aware that admittance controls are unstable if tuned too aggressively and can cause oscillations in the system by hitting self-resonance when under-damped. Therefore, we experimentally tune the admittance value in a series of force holding tasks to find a reasonable value for the admittance that gives good response time, close to what could be considered critical damping or slightly overdamped. To test this, we repeat the Simple Force Holding task with various values of admittance. For our testing case the admittance matrix, \mathbf{A} , is a scalar matrix equal to $A\mathbf{I}$, where A is the tuned scalar

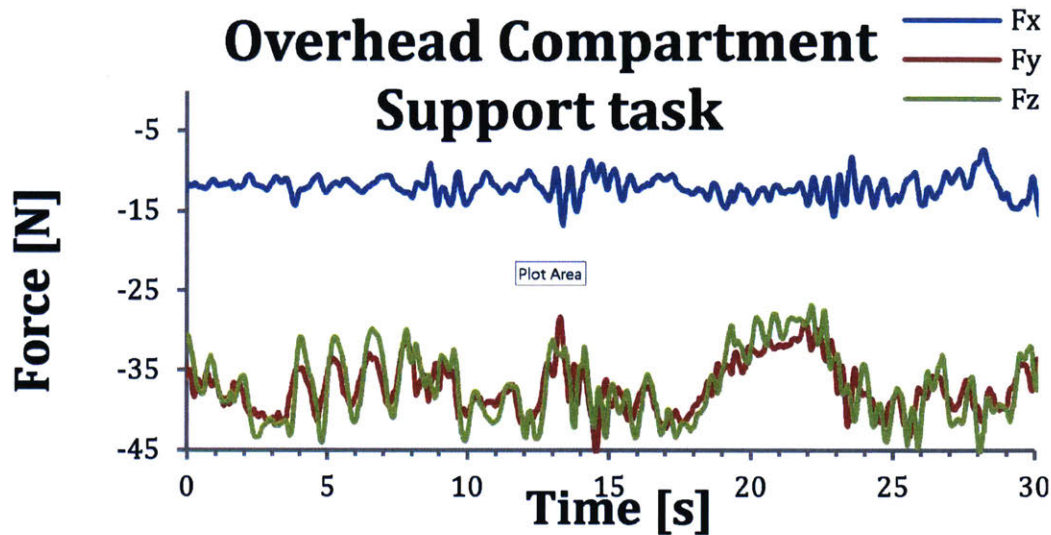


Figure 7-3: Force Measured During The Overhead Compartment Task (Admittance = 0.04 m/s/N)

value of admittance in $\frac{\text{m/s}}{\text{N}}$. The wearer is instructed to rhythmically move back and forth to force the system with an input disturbance of some frequency to see if this causes instability or if the damping is too large at that point such that it restricts the movement of the wearer.

Figure 7-4 shows the force output deviation from the set point force for various admittances, A , ranging from $0.10 \frac{\text{m/s}}{\text{N}}$ to $0.013 \frac{\text{m/s}}{\text{N}}$. For values of $A > 0.05 \frac{\text{m/s}}{\text{N}}$ the system is underdamped, and while the $0.1 \frac{\text{m/s}}{\text{N}}$ controller has fast response with less force deviation, it begins to oscillate wildly when the wearer moves back and forth, this is from the inherent instability of the admittance controller, the admittance loop resonates with its output, causing greater measured force disturbance that it tries to compensate. For values of admittance above the optimally performing $0.04 \frac{\text{m/s}}{\text{N}}$, the robot arm was overdamped. This was especially clear at $0.013 \frac{\text{m/s}}{\text{N}}$ where the wearer was required to input an excessive amount of force to move the SRL. This is marked in the data by an increase in the amplitude and offset of the force deviation required to move the SRL, look to Figure 7-4 where the force deviations in $A = 0.02$ and $A = 0.013$ are larger in magnitude than those of the ultimately selected value of

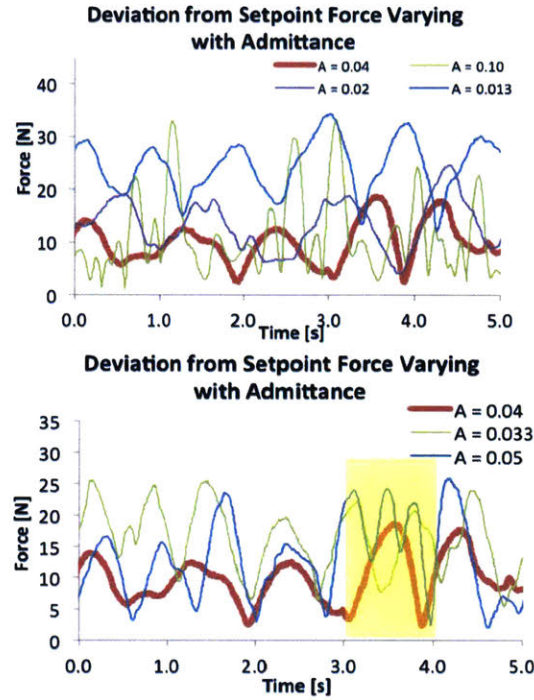


Figure 7-4: Forces Measured for Various Admittance Values, for the Tuning of the Admittance Parameter

$0.04 \frac{m/s}{N}$. Around the optimal point of $0.04 \frac{m/s}{N}$, also test values of 0.033 and 0.05: in Figure 7-4 the amplitude of force deviation is again greater for the lower value of admittance, and, as well for some points the slightly increased admittance of $0.05 \frac{m/s}{N}$ became unstable as shown in the highlighted region. We note then that we have found a well-balanced value of admittance at $0.04 \frac{m/s}{N}$ as it is the highest admittance value tested that is not prone to instability, approximating our goal of near critical damping.

7.4 Postural Compensation and Tracking of the World Coordinates

One of the major features of the control algorithm is to allow for the worker to move freely, and have the robot track this motion to compensate and control the force applied in the direction of the world coordinate system specifically. The 9-DOF IMU

used allows the SRL control loop to track the roll, pitch, and yaw of the base of the robot and thereby the human worker. Figure 7-5. shows that in a force holding task, the orientation (being the pitch and yaw about the fixed axes) of the worker changes, yet the force in the world coordinates remains set point about the world coordinates. Figure 7-5. also shows that the oscillations in the force for the well-tuned system match with the desired input velocity nicely, matching the velocity with the appropriate admittance of a virtual damper, as the model of admittance control would suggest.

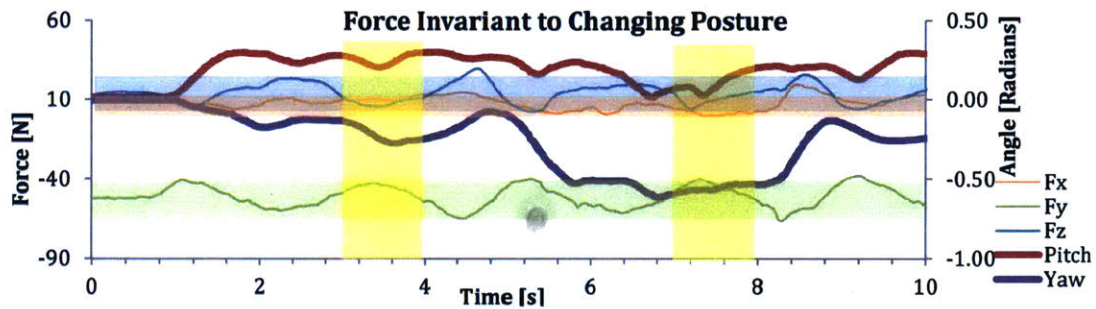


Figure 7-5: Force and IMU Data During a Force Holding Task

Figure 7-8 shows data from a trial where the robot was attempting to stay in alignment with the x-axis. As the wearer yaws or rotates about the Z-axis, the shoulder joint, θ_1 rotates to compensate. This is a strong indicator of good tracking as yaw is typically the hardest orientation to track with an IMU, as it is perpendicular to gravity, and so only the compass and the accelerometer can track the yaw. This data shows little time delay and the offset is only a result of the mounting of the motor, being present since the start of the data collection. Our results also suggest that the control algorithm is effective at keeping the force compensation pointed in the world coordinate system. In Figure 7-5. the Pitch and Yaw vary over time, but when the forces are measured in the world coordinate frame, they only change to account for the velocity changes. Note the rapid change in yaw between 5 and 6 seconds. Here, no drastic change in the forces is observed, demonstrating effective compensation for postural changes when coupled with the data from Figure 7-8. The colored bands in Figure 7-5 show the range of values and highlight that the amplitude

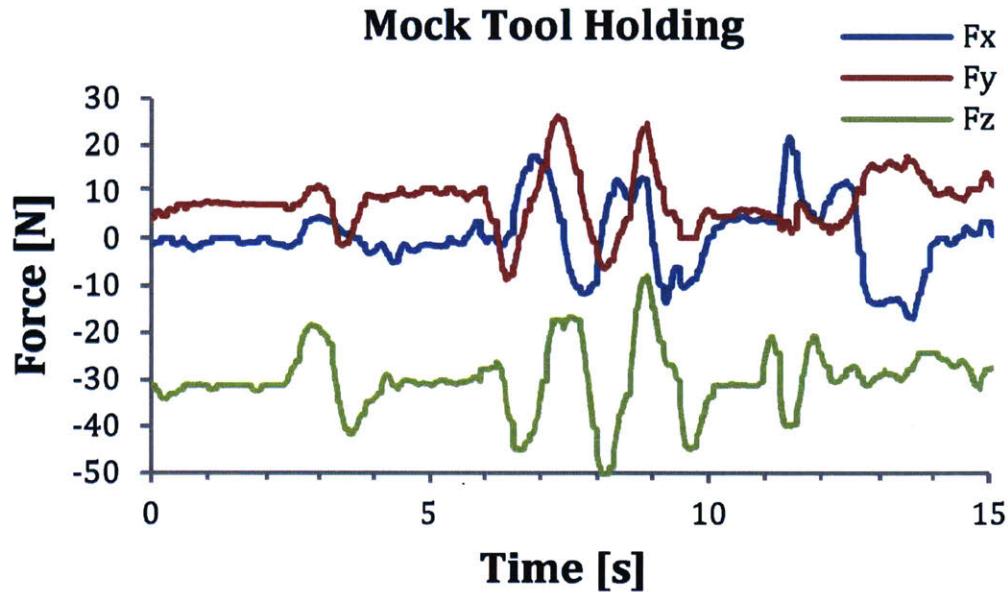


Figure 7-6: Force Measured During a Tool Supporting Trial (Admittance = 0.04m/s/N)

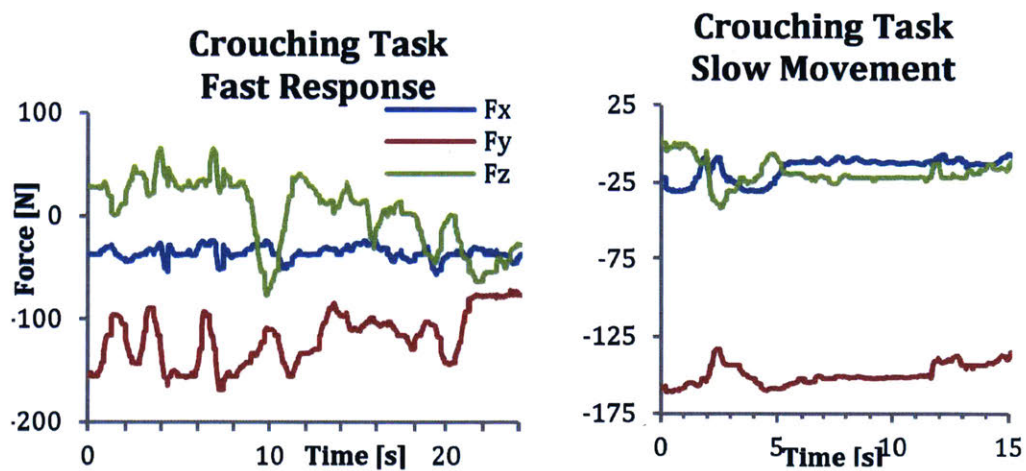


Figure 7-7: Force Measured During a Worker Prone Supporting Trial (Admittance = 0.04m/s/N)

or offset of the oscillations do not change with changing Pitch or Yaw. Compare the regions of 3-4s vs 7-8s where the difference in Yaw is 0.30 radians or almost 20deg .

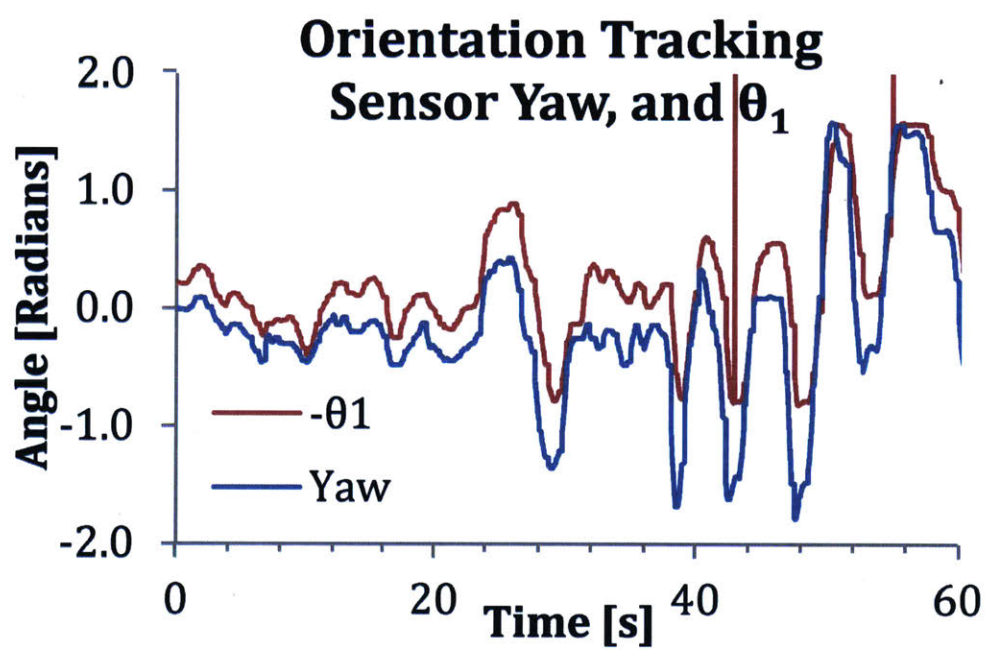


Figure 7-8: Orientation and Position Data During Vector Following Trial; the two angles are complimentary: as θ_1 rotates the shoulder to compensate for the change in Yaw. Shown here is the Yaw angle and negative θ_1

Chapter 8

Conclusion and Future Works

An improved design of Supernumerary Robotic Limbs is presented in addition to the design of a novel ergonomic attachment that is used to interface the SRL with the wearer. We also present a novel use case and some design changes to the universal granular jamming gripper. A closed loop implementation of force control allows the wearer to move and perform dynamic tasks while the SRL holds workpieces overhead as well as accomplish many other tasks. The control scheme presented yields a natural and intuitive interface for SRL interaction that is also effective and versatile.

Our results demonstrate a flexibility of tasks that can be completed with the simple and robust force control loop. We as well have demonstrated a successful implementation of orientation/postural compensation for human-worn robotic systems that is very responsive and reliable to the tests conducted. The overall system is fairly lightweight, low cost, and requires fairly low computational power to run successfully. We hope that this work could be expanded into a future work-ready implementation that increases safety, robustness, and reliability.

Other future work to be explored may include tighter integration of this force control scheme with direct/inferred control, and increased control complexity. As well, we believe that future work can allow for direct control using similarly intuitive feedback to give more natural interactions that make the SRLs more akin to an extension of the human body as opposed to a worn robotic arm. The ultimate goal of this sort of research is truly to augment human capability in intuitive ways.

Bibliography

- [1] Bureau of Labor Statistics, *2015 Nonfatal Occupational Injuries and Illnesses: Cases with days away from work*, Bureau of Labor Statistics, 2016.
- [2] British Airways. “British Airways - Building the 787-9 Dreamliner.” Online video clip. YouTube. YouTube, Sep 30, 2015. Web. 15 Nov, 2015.
- [3] Lockheed Martin. FORTIS EXOSKELETON - RELIEF FOR THE DAILY GRIND. N.p.: Lockheed Martin, 2016. Lockheed Martin, 2016. Web. 15 Jan. 2017.
- [4] Altenburger, Ruprecht, Daniel Scherly, and Konrad S. Stadler. *Design of a Passive, Iso-elastic Upper Limb Exoskeleton for Gravity Compensation*. ROBOMECH Journal 3.1 (2016).
- [5] L. Martin, “Relief for the Daily Grind: Industrial Exoskeletons at Work”, 2014.
- [6] CYBERDYNE. “The World’s First Cyborg-type Robot” HALÂŕ - CYBERDYNE. CYBERDYNE Inc., 2017. Web. 15 Jan. 2017.
- [7] R. A. R. C. Gopura and K. Kiguchi, *Mechanical designs of active upper-limb exoskeleton robots: State-of-the-art and design difficulties*, 2009 IEEE International Conference on Rehabilitation Robotics, Kyoto International Conference Center, 2009, pp. 178187.
- [8] J. C. Perry and J. Rosen, *Design of a 7 Degree-ofFreedom Upper-Limb Powered Exoskeleton*, The First IEEE/RAS-EMBS International Conference on Biomedical Robotics and Biomechatronics, 2006. BioRob 2006., Pisa, 2006, pp. 805-810.

- [9] A. Schiele and F. C. T. van der Helm, *Kinematic Design to Improve Ergonomics in Human Machine Interaction*, in IEEE Transactions on Neural Systems and Rehabilitation Engineering, vol. 14, no. 4, pp. 456-469, Dec. 2006.
- [10] F. Parietti and H. Asada, "Dynamic analysis and state estimation for wearable robotic limbs subject to human induced disturbances," in Proc. IEEE Int. Conf. Robot. Autom., 2013, pp. 3880-3887.
- [11] F. Parietti and H. Asada, "Supernumerary robotic limbs for aircraft fuselage assembly: Body stabilization and guidance by bracing," in Proc. IEEE Int. Conf. Robot. Autom., 2014, pp. 1176-1183.
- [12] F. Parietti and H. Asada, "Supernumerary Robotic Limbs for Human Body Support", IEEE Transactions on Robotics, Vol.32, No.2, pp301-311, 2016.
- [13] F. Parietti, K. Chan, and H. Asada, "Bracing the human body with supernumerary robotic limbs for physical assistance and load reduction," in Proc. IEEE Int. Conf. Robot. Autom., 2014, pp. 141-148.
- [14] D. Kurek and H. Asada, "The MantisBot: Design and Impedance Control of Supernumerary Robotic Limbs for Near-Ground Work", to appear in Proceedings of the 2017 IEEE International Conference on Robotics and Automation, 2017
- [15] F. Wu and H. Asada, *Implicit and Intuitive Grasp Posture Control for Wearable Robotic Fingers: A DataDriven Method Using Partial Least Squares*, IEEE Transactions on Robotics, vol. 32, no. 1, pp. 176-186, 2016.
- [16] B. L. Bonilla and H. H. Asada, *A robot on the shoulder: Coordinated human-wearable robot control using Coloured Petri Nets and Partial Least Squares predictions*, International Conference on Robotics and Automation (ICRA), pp. 119-125, 2014.
- [17] Llorens-Bonilla, B., Parietti, F., and Asada, H. H., "Demonstration-based control of supernumerary robotic limbs," In Intelligent Robots and Systems (IROS), 2012 IEEE/RSJ International Conference on. IEEE, pp. 3936-3942, 2012.

- [18] Llorens-Bonilla B, Asada H. Control and Coordination of Supernumerary Robotic Limbs Based on Human Motion Detection and Task Petri Net Model. ASME. Dynamic Systems and Control Conference, Volume 2: Control, Monitoring, and Energy Harvesting of Vibratory Systems; Cooperative and Networked Control; Delay Systems; Dynamical Modeling and Diagnostics in Biomedical Systems; Estimation and Id of Energy Systems; Fault Detection; Flow and Thermal Systems; Haptics and Hand Motion; Human Assistive Systems and Wearable Robots; Instrumentation and Characterization in Bio-Systems; Intelligent Transportation Systems; Linear Systems and Robust Control; Marine Vehicles; Non-holonomic Systems ():V002T27A006. doi:10.1115/DSCC2013-4083.
- [19] Llorens-Bonilla, Baldin Adolfo. "Supernumerary Robotic Limbs : Task Planning, Execution, and Prediction-based Coordination with the Human Wearer." Thesis. Massachusetts Institute of Technology, 2013. Supernumerary Robotic Limbs : Task Planning, Execution, and Prediction-based Coordination with the Human Wearer. Massachusetts Institute of Technology, Sept. 2013. Web. Mar. 2016. <<https://dspace.mit.edu/handle/1721.1/85487>>.
- [20] Sengeh, David Moinina, and Hugh Herr. "A Variable-Impedance Prosthetic Socket for a Transtibial Amputee Designed from Magnetic Resonance Imaging Data." JPO Journal of Prosthetics and Orthotics 25.3 (2013): 129-37. Web.
- [21] Georgia Tech. "Robot allows musicians to become three-armed drummers." Online video clip. YouTube. YouTube, Feb 17, 2016. Web. Mar 6, 2016.
- [22] H. Kim, L. M. Miller, A. Al-Refai, M. Brand and J. Rosen, "Redundancy resolution of a human arm for controlling a seven DOF wearable robotic system," 2011 Annual International Conference of the IEEE Engineering in Medicine and Biology Society, Boston, MA, 2011, pp. 3471-3474.
- [23] Pan G., Fu H., Zhang X., Ma F. (2017) Research on Bionic Mechanism of Shoulder Joint Rehabilitation Movement. In: Yang C., Virk G., Yang H. (eds) Wearable

Sensors and Robots. Lecture Notes in Electrical Engineering, vol 399. Springer, Singapore

- [24] B. Siciliano and O. Khatib (ed.), “Handbook of Robotics”, Part A Robotics Foundations, Springer, 2008.
- [25] E. Brown, N. Rodenberg, J. Amend, A. Mozeika, E. Steltz, M. Zakin, H. Lipson, H. M. Jaegera, “Universal robotic gripper based on the jamming of granular material”, PNAS, 107(44): pp. 18809–18814, 2010.
- [26] J. Amend, E. Brown, N. Rodenberg, H. Jaeger and H. Lipson, *A Positive Pressure Universal Gripper Based on the Jamming of Granular Material*, IEEE Transactions on Robotics, vol. 28, no. 2, pp. 341-350, 2012.
- [27] N. G. Cheng et al., *Design and Analysis of a Robust, Low-cost, Highly Articulated manipulator enabled by jamming of granular media*, 2012 IEEE International Conference on Robotics and Automation, Saint Paul, MN, 2012, pp. 4328-4333.
- [28] J. Kapadia and M. Yim, *Design and performance of nubbed fluidizing jamming grippers*, 2012 IEEE International Conference on Robotics and Automation, Saint Paul, MN, 2012, pp. 5301-5306.
- [29] T. Nishida, D. Shigehisa, N. Kawashima and K. Tadakuma, *Development of universal jamming gripper with a force feedback mechanism*, 2014 Joint 7th International Conference on Soft Computing and Intelligent Systems (SCIS) and 15th International Symposium on Advanced Intelligent Systems (ISIS), Kitakyushu, 2014, pp. 242-246.
- [30] R. R. Ma, L. U. Odhner and A. M. Dollar, *A modular, open-source 3D printed underactuated hand*, 2013 IEEE International Conference on Robotics and Automation, Karlsruhe, 2013, pp. 2737-2743.
- [31] G. P. Jung, J. S. Koh and K. J. Cho, *Underactuated Adaptive Gripper Using Flexural Buckling*, in IEEE Transactions on Robotics, vol. 29, no. 6, pp. 1396-1407, Dec. 2013.

- [32] Y. Nakamura and H. Hanafusa, *Inverse Kinematic Solutions With Singularity Robustness for Robot Manipulator Control*, Journal of Dynamic Systems, Measurement, and Control, vol. 108, no. 3, p. 163, 1986.
- [33] Ordóñez, Francisco, and Daniel Roggen. "Deep Convolutional and LSTM Recurrent Neural Networks for Multimodal Wearable Activity Recognition." *Sensors* 16.1 (2016): 115. Web.
- [34] Roggen, Daniel, Alberto Calatroni, Mirco Rossi, Thomas Holleczech, Kilian Forster, Gerhard Troster, Paul Lukowicz, David Bannach, Gerald Pirkel, Alois Ferscha, Jakob Doppler, Clemens Holzmann, Marc Kurz, Gerald Holl, Ricardo Chavarriaga, Hesam Sagha, Hamidreza Bayati, Marco Creatura, and Jose Del R. Millan. "Collecting Complex Activity Datasets in Highly Rich Networked Sensor Environments." *2010 Seventh International Conference on Networked Sensing Systems (INSS)* (2010): n. pag. Web.
- [35] Satoshi Suzuki, Keiichi Abe. Topological structural analysis of digitized binary images by border following. *Computer Vision, Graphics, and Image Processing*, 30(1):32–46, 1985.
- [36] Zoccolan, D., Graham, B. J., & Cox, D. D. (2010). A Self-Calibrating, Camera-Based Eye Tracker for the Recording of Rodent Eye Movements. *Frontiers in Neuroscience*, 4, 193. <http://doi.org/10.3389/fnins.2010.00193>